Journal of Archaeological Science 140 (2022) 105546

Contents lists available at ScienceDirect

Journal of Archaeological Science

journal homepage: www.elsevier.com/locate/jas

Exotic glass types and the intensity of recycling in the northwest Quarter of Gerasa (Jerash, Jordan)

Gry H. Barfod [a,b], Ian C. Freestone [c], Ruth E. Jackson-Tal [d], Achim Lichtenberger [e], Rubina Raja [b,f,*]

[a] Aarhus Geochemistry and Isotope Research (AGiR) Platform, Department of Geoscience, Aarhus University, DK-8000, Aarhus C, Denmark
[b] The Danish National Research Foundation's Centre of Excellence Centre for Urban Network Evolutions, Aarhus University, DK-8260, Hojbjerg, Denmark
[c] UCL Institute of Archaeology, London, WC1H 0PY, United Kingdom
[d] The Israel Museum, Jerusalem, 9171002, Israel
[e] Institut für Klassische Archäologie und Christliche Archäologie, Münster University, Münster, Germany
[f] School of Culture and Society, Aarhus University, DK-8000, Aarhus C, Denmark

ARTICLE INFO

Keywords:
Gerasa
Glass analysis
Trade
Production
Recycling intensity
Roman and Byzantine glass

ABSTRACT

Major and trace elements are presented for 149 glass fragments ranging in date from the Roman to Early Islamic periods (1st – mid-8th centuries CE), excavated during the Danish-German Jerash Northwest Quarter Project's fieldwork between 2011 and 2016. The results confirm a clear dominance of Levantine glass types, but also reveal 12 glasses of Egyptian and Mesopotamian compositions recovered from two houses destroyed by the major earthquake which hit parts of the Levant in January 749 CE. These closed and undisturbed contexts from the final phase of occupation reveal the presence of relatively more pristine Levantine as well as imported material that is less visible in earlier contexts in the Gerasa assemblage, where the recycling indexes are high and chemical signatures of any exotic glass were largely lost due to remelting and their dilution by the overwhelming quantities of glass produced in the Levantine region. This emphasizes that imported glass may frequently be underestimated or even invisible in glass compositional studies, depending on the archaeological context sampled and the approach taken to artifact quantification.

Levantine glass was attributed to Roman, Late Roman (Jalame) and Byzantine/Early Islamic (Apollonia) productions based primarily on MnO, Al_2O_3 and Na_2O concentrations, which offered an advantage over previous approaches. While colorants in weakly colored glass indicate recycled material, their concentrations are sensitive to context, with higher concentrations in the early periods when the use of intentionally colored glass was more frequent. We have therefore developed the concept of the intensity of recycling, which was estimated using components modified during prolonged melting, such as K_2O, P_2O_5 and Cl. A pronounced enrichment in CaO, also dependent upon the intensity of recycling, may affect the assignment to compositional groups and should be taken into consideration in future. Recycling in Gerasa appears to have been more intensive than was the case for cities closer to the primary production centers on the Mediterranean coast, consistent with the view that the dependency on recycling increases further away from the source of the primary material. In contrast, the cities in the coastal plain could readily exploit the marine transportation network, which appears to have played a major role in the distribution of raw glass. (361 words).

1. Introduction

The glass-making centers on the coast of the eastern Mediterranean appear to have dominated production during the first millennium CE, and numerous elemental and isotopic analyses have shown raw glass from Levantine and Egyptian production centers to have been distributed to secondary workshops across the Roman and Late Antique worlds, where it was re-melted and shaped into functional artifacts (e.g. Barfod et al., 2020; Bidegaray et al., 2019; Ceglia et al., 2015; Degryse, 2014; Freestone et al., 2018; Ganio et al., 2012a, 2012b; Schibille et al.,

* Corresponding author. The Danish National Research Foundation's Centre of Excellence Centre for Urban Network Evolutions, Aarhus University, DK-8270, Hojbjerg, Denmark.
E-mail address: rubina.raja@cas.au.dk (R. Raja).

https://doi.org/10.1016/j.jas.2022.105546
Received 12 May 2021; Received in revised form 6 December 2021; Accepted 15 January 2022
Available online 16 February 2022

2017; Silvestri et al., 2008). Traded material clearly has the potential to provide insights into the ancient economy (Wilson and Bowman, 2018), but interpretation of recovered glass in any detailed way is complex due to the fact that glass was readily recycled (Freestone, 2015; Jackson and Paynter, 2016; Paynter and Jackson, 2016; Silvestri 2008) and any recovered assemblage therefore likely to represent a mixture of fresh and recycled glass. Furthermore, "recycled glass", which is typically identified by raised levels of contaminating colorant elements, may incorporate material that has been broken and re-melted just once or twice, or has gone through a large number of cycles. The determination of the *intensity* of glass recycling, at least in relative terms, is therefore an issue of key importance in the interpretation of the glass economy. An additional issue which is not commonly addressed is the extent to which glass vessels, as opposed to raw glass material, were traded over long distances. As the composition of a glass vessel primarily reflects that of the primary raw glass production site, rather than the workshop in which it was made, it does not readily allow discrimination between these two interpretations.

To obtain a more nuanced understanding of glass production and consumption requires detailed and comprehensive investigations of well-contextualized assemblages, as well as the development of new approaches to the understanding of issues such as recycling. Our provisional investigation of a small sample from a larger assemblage of Roman and Byzantine glass excavated at the Northwest Quarter in Gerasa (modern Jerash) in Jordan (Barfod et al., 2018) suggested that this assemblage has the potential to help unravel some of these problematic issues, and work on the Jerash assemblage has also allowed us to introduce the study of the isotopes of hafnium to discriminate between glass made in the Levant and Egypt (Barfod et al., 2020). In the present paper we present the results of a major campaign of elemental and isotopic analysis, specifically aimed to further our understanding of the role of glass supply and recycling in the economy of the ancient city and their roles relative to cities in other parts of the Levant. This large dataset allows us to develop new approaches for the attribution of glass to different Levantine production centers and to develop the concept of "recycling intensity", whereby we are able to compare recycling practices in different assemblages. The new evidence, along with the information from other Jerash glass studies (Baldoni, 2019; Barfod et al., 2018; Barfod and Søgaard, forthcoming; Baur, 1938; Bobou and Krag, forthcoming; Boschetti et al., 2021; Boschetti and Wootton, in press; Jackson-Tal, 2021; Kraeling, 1938), sheds light on the extensive use of glass at the site and provides evidence for the considerable, diverse, and continuous use of glass vessels in everyday life, especially during the Late Roman, Byzantine, and Early Islamic (Umayyad) periods.

2. Locality and sample selection

The ancient city of Gerasa, located north of Jordan's modern capital Amman (ancient Philadelphia), belonged to the Decapolis, a group of Greco-Roman cities which exercised a substantial degree of autonomy (Fig. 1a). Founded during the Hellenistic period (2nd century BCE), the city developed under Roman rule and became an urban center, typical for the Roman Eastern Mediterranean (Kraeling, 1938; Zayadine, 1986; Lichtenberger and Raja, 2018a). The city prospered during the Late Roman, Byzantine and Early Islamic periods until an earthquake in 749 CE led to its demise and abandonment (Bes et al., 2020; Lichtenberger and Raja, 2019a).

During the Roman and Late Antique periods, Gerasa was a medium-sized city incorporating the typical urban architectural inventory of a provincial Roman imperial city (Raja, 2012). It relied on a fertile and water-rich hinterland that was exploited agriculturally (Boyer, 2018; Lichtenberger and Raja 2019a). Especially along the Wadi Jerash, which originated 12 km northwest of the urban center and flowed into the Wadi az-Zarqa (the Biblical Jabbok), intensive terracing took place for agriculture purposes. There are indicators that these terraces declined from as early as the 6th century CE onwards and the agricultural areas

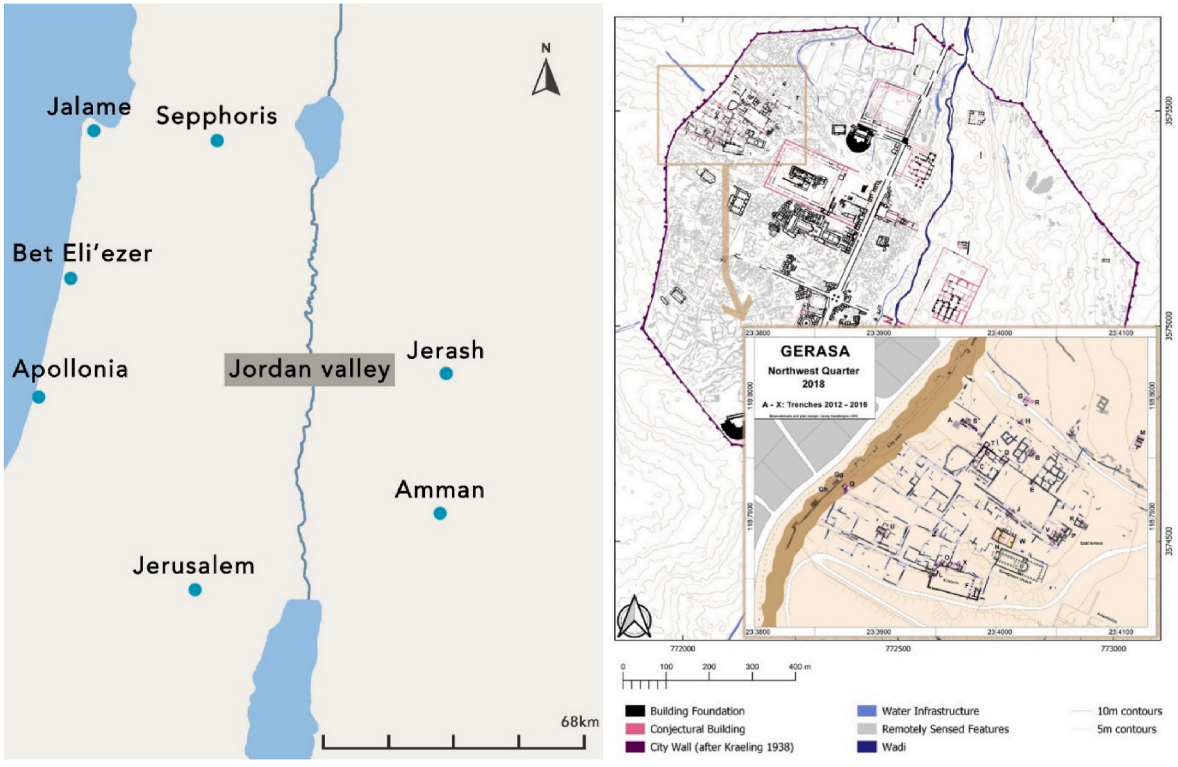

Fig. 1. a. Regional map of the Southern Levant showing the locations of Gerasa (Jerash) in N. Jordan, glass production sites at Jalame and Apollonia and the cities of Sepphoris and Jerusalem to the west of the Jordan Valley. b. Map of Gerasa and the NW Quarter showing trenches from the 2011–2016 Danish-German Jerash Northwest Quarter Project excavations. Trench K contains the remains of the earthquake-stricken 'House of the Scroll' where 35 of the 149 sherds in this study were found.

were no longer managed to the previous degree (Lichtenberger et al., 2019, 2021). However, within the city center, there are no obvious signs of urban decline during this period, and there is evidence of numerous constructions of churches and intensive urban encroachment. Despite not being located on the main roads in the region, Gerasa was tied well into the infrastructure of the region, including the road network, which led to the coast of the Mediterranean and along a major south-north route from the Arabian Peninsula to Mesopotamia. A minor road network provided high connectivity on a regional level within the Decapolis (Kennedy, 2007).

From at least the Roman period, the city was a pottery production center that produced many products for domestic use but also for regional export (Lichtenberger and Raja, 2018b, 2019b, 2020; Romanowska et al., 2021a,b,); other crafts, as attested by inscriptions, included gold-smithing (Welles, 1938). This urban economy thrived until the earthquake of 749 CE hit the city on the morning of 18th January.

Glass-working at Gerasa is attested by earlier archaeological evidence from the so-called Glass Court and Fountain Court close to the Christian cathedral. In this area, heaps of broken glass collected for remelting were excavated, suggesting an active recycling industry (Baur, 1938). However, the associated cakes of colored glass need not represent glass melting on site, as was implied (Bauer, op. cit.). They are present at other sites in the region (Marii and Rehren, 2009, 2012) and may represent the trade in cakes of colored glass intended to be broken into tesserae for the production of mosaics, which is known from across the ancient world (e.g. Paynter et al., 2015). That secondary glass manufacturing did take place in Jerash is however implied from glass-working shops within the Sanctuary of Artemis (Baldoni, 2019). Although no glass furnaces were recovered here, the presence of 'deformed glass vessels, glass chunks and lumps' as well as crucible fragments 'with layers of melted glass of varying thickness adhering to the bottom of the bowls' yield evidence of glass-working activities here (Baldoni, 2019).

Samples for the present study come from excavations undertaken by a Danish-German team in the Northwest Quarter of the city (https://doi.org/10.6084/m9.figshare.12116286). The Northwest Quarter is the highest area within the city, situated to the West of the Roman Artemision and to the Northwest of the Late Antique ecclesiastical structures around the so-called cathedral complex (Fig. 1b). The structures in the Northwest Quarter consisted mainly of domestic complexes from Late Roman to Early Islamic times but also infrastructural complexes such as cisterns and oil presses as well as a Late Antique synagogue, which in the 6th century was turned into a church complex (Fig. 1b: Lichtenberger and Raja, 2018a; 2018b; 2018c). The area is an intensively studied urban context given the vast material that has been contextualized on site and subsequently studied using a wide variety of geo-physical, typological, and chemical methods (e.g. Lichtenberger and Raja, 2018a, 2018b, 2019a, 2019b, 2020; Stott et al., 2018; Lichtenberger et al., 2019; Barfod et al., 2020). From these results, a detailed picture of the settlement history and the inner workings of this part of the city has emerged.

The excavation has taken a full quantification approach to all finds. Ceramics, unsurprisingly, make up the largest group, amounting to about 800,000 sherds. However, numerous artifacts of glass, metal, as well as bone make up a significant component. Around 5500 glass fragments were unearthed, of which about 1740 were diagnostic (Jackson-Tal, 2021). They represent a wide range of functions in daily life: tableware used for serving, dining, and storing foods; vessels used as containers of cosmetic substances; lighting, namely vessels used as lamps and windowpanes; jewelry and small finds used as inlays, for spinning wool, and mosaic tesserae (Jackson-Tal, 2021). The glass typologies have many parallels in the region, and therefore on the whole they are likely to have been locally made. Some remains of glass-vessel production were found in several trenches on the site, including glass lumps; drops, deformed pieces, and trails; small, angular raw glass chunks; and the remains of ceramic vessels with glazed layers, which appear to be crucibles for glass melting similar to the fragments from the Sanctuary of Artemis reported by Baldoni (2019; see above) to the west of the Northwest Quarter.

2.1. The earthquake-stricken houses in trenches K and P

Forty-two of the glass sherds in this study (thirty-five from trench K and seven from trench P) come from closed contexts within two domestic building complexes destroyed in the 749 CE earthquake (Lichtenberger et al., 2016). The event is confirmed by the character of the destruction of the houses and their dates obtained from pottery, carbon 14 dating, coins, and other finds. The first Umayyad-period complex, located in trench K (Fig. 1b; Tables A1–3) and referred to as the House of the Scroll was constructed directly on bedrock during the Early Islamic period with no Byzantine-period predecessor. The finds are thus a deposit of the inventory of the house as it was when the catastrophic event of the earthquake hit and include among other things a silver scroll with pseudo-Arabic text, a small coin hoard, a mortar with pestle, a comb, beads of agate, carnelian and glass, as well as two intact glass bottles measuring about 10 cm in height (Kalaitzoglou et al., 2015; Lichtenberger et al., 2016; Lichtenberger and Raja, 2019c; Orfanou et al., 2020). Most of the glass fragments were concentrated in a 1.5–2 m silty clay debris layer (evidences 3, 7, 35, 39, 44) that originated from the collapsed upper stories. These can be identified from the sample numbers consisting of four parts referring to 1. the Jerash excavation season, 2. the trench and the respective sector (Fig. 1b), 3. the evidence number, and 4. the single find number; e.g. find number J14-Kc-3-59 was excavated during the 2014 excavation season from sector c in trench K within evidence 3 and is counted as find number 59.

In the second Umayyad-period complex referred to as House of the Tesserae, the finds of blocks with regular cut marks and incisions as well as a trough with unused white tesserae suggest that it was undergoing reconstruction when the earthquake struck (Lichtenberger and Raja, 2017). Like the House of the Scroll, this house was arranged with rooms in several stories that had no Byzantine-period predecessor and consisted of ground-floor rooms with more practical functions such as e.g. a kitchen (Lichtenberger and Raja, 2017). The glass finds and mosaic fragments from the collapsed upper stories were found in yellowish soil layers (evidences 5, 15, 16) within these lower rooms that correspond to the silty clay destruction layers from House of the Scroll (Lichtenberger and Raja, 2017).

2.2. Typology

In total, 149 fragments from vessels and small objects from the NW Quarter excavations were analyzed. These include sagged, free-blown, and mould-blown bowls, bottles and jugs, wine-glasses, lamp bowls, kohl tubes, and windowpanes. Most vessels are plain, but some are decorated with wheel-cut or mould-blown designs: vertical ribs, indents, applied and tooled trails, pinches, discs, and blobs (Fig. 2; Jackson-Tal, 2021). The small finds include beads, bracelets, a stirring rod, inlays, a spindle whorl, and mosaic tesserae (Jackson-Tal, 2021). The great majority can be dated to the main stages of occupation at the site during the Late Roman, Byzantine, and Umayyad periods, from the third to the eighth century CE.

A few finds can be dated to the Late Hellenistic and Early Roman periods, from the mid-second century BCE to the early second century CE. The vessels and small finds were made mostly of colorless glass, but also light green, light and dark blue, bluish-green, light yellow, yellow-brown, yellow-green, and purple glass appear. They are covered in a thick black, silver, and white weathering and an iridescent film. Table A2 lists all objects, their typologies, as well as chronological contexts.

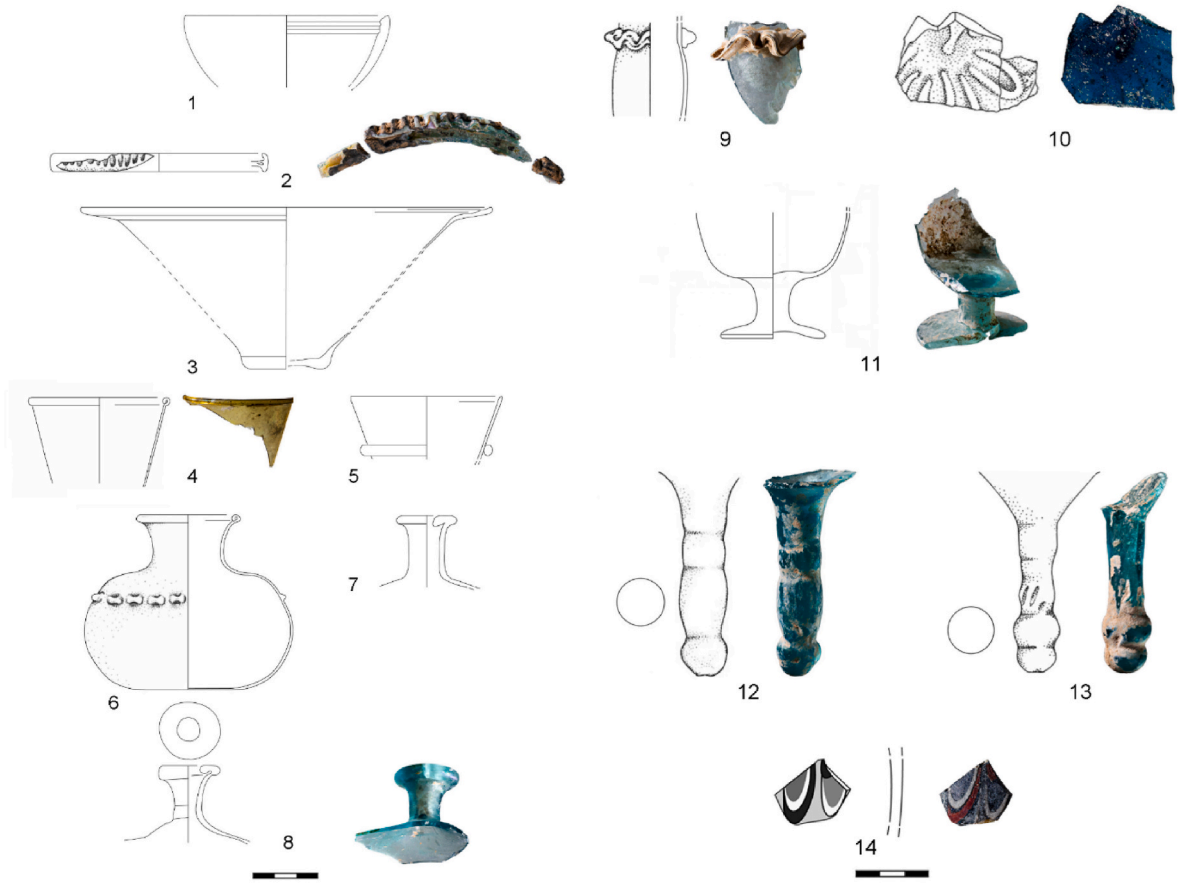

No.	Loci	Vessel Type	Date	Glass Type
1	J13-Ha/Ha1-13-50	Grooved bowl	Hell/Early Roman	Rom SbMn
2	J15-Qac-41-11	Bowl with crimped trail	Early Roman	Plant Ash-1
3	J14-Jd-32-154	Bowl with splaying-out rim	Early Islamic	Rom Sb
4	J15-Pe-15-35	Bottle with folded-in rim	Early Islamic	Apollonia-type
5	J15-Ob-107-4a	Bottle with funnel-shaped trailed rim	Byzantine/ Early Islamic	Rom Mn-type
6	J14-Kg-39-14	Bottle w. horizontal pinches	Early Islamic	Apollonia-type
7	J15-Ob-107-4b	Bottle with folded-in rim	Byzantine/ Early Islamic	Rom Mn-type
8	J15-Oi-97-6	Bottle with folded-in rim	Early Islamic	Apollonia-type
9	J14-Kc-3-117	Bottle with wavy trail	Early Islamic	Apollonia-type
10	J14-Kc-43-5	Mold-blown bottle	Early Islamic	Plant Ash-2
11	J13-Fi-0-14	Wine-glass	Byzantine	Apollonia-type
12	J14-Kh-24-3	Stemmed lamp bowl	Byzantine/ Early Islamic	Apollonia-type
13	J14-Kg-3-235	Stemmed lamp bowl	Byzantine/ Early Islamic	Apollonia-type
14	J14-Kd-46-7	Marvered wall fragment	Early Islamic	Apollonia-type

Fig. 2. Examples of typologies and their chronologies in this study.

3. Methods

3.1. Electron microprobe – EMP

Small chips (1 mm × 1mm) of fresh glass were mounted in epoxy and polished down to 1 μm to avoid sodium loss on altered surfaces (e.g. Duckworth et al., 2015). Spot analyses were performed on a JEOL JXA8500F with five wavelength dispersive spectrometers (WDS) at Washington State University GeoAnalytical Lab using NIST glasses, natural minerals and synthetic minerals for calibration. Analytical settings during the analyses included acceleration voltage of 20 kV, beam current of 10 nA and 10 μm beam size. Peak count times varied from 160 s for MgO down to 10 s for Na_2O, SiO_2 and Al_2O_3. Compositions were corrected for intensity following the ZAF procedure, for interferences following Donovan et al. (1993), for backgrounds following Donovan and Tingle (1996), and for elemental migration due to beam damage following Nielsen and Sigurdsson (1981). Accuracies were estimated by repeated analysis of Corning Museum Archaeological glass standards, CorB (n = 149) and CorD (n = 151) and were generally within ≤5% relative of known values for element concentrations ≥0.2 wt% (Table A1). Exceptions included Na_2O and TiO_2 concentrations below 1.5 and 0.1 wt%, respectively, which deviated from known Corning standard values by 13% (Na_2O) and 22% (TiO_2) (Table A1). Accuracies were also found to be low for PbO and, to a lesser degree, for CuO (Table A1) and, for this reason, ICP-MS analyses for these two elements are used in figures, discussion, and interpretations. Table A2 reports sample analyses as means of 6 repeats.

3.2. Laser ablation (LA)-ICPMS

Analysis for 44 trace elements was done at the AGiR (Aarhus Geochemistry and Isotope Research) platform using an Agilent 7900 quadrupole ICP-MS coupled to a Resonetics 193 nm laser ablation instrument. Laser settings were laser energy at 80 mJ, 300 μm line scans, 60 μm spot size, 10 Hz repetition rate and acquisition time of 71 s. Data reduction was done using Iolite software as well as offline with USGS glass standard GSE-G1 as calibration standard by matching sample Si counts to the SiO_2 concentrations obtained from EMP analyses. Accuracies were estimated from repeated analysis of USGS glass standard GSD-G1 (n = 18) showing concentrations within 5% of known values for most elements (Table A3). Table A3 reports sample analyses as means of 5 repeats.

3.3. Multi-collector ICPMS

Hafnium, strontium, and neodymium isotope analysis were done for 5 plant-ash glasses on the Nu Plasma II MC-ICPMS using a DSN nebulizer at AGiR (Table A4). Details on sample preparation, MC-ICPMS run conditions and standard isotope analyses are in Barfod et al. (2020).

4. Results: Sources and chronology

The 149 fragments are soda-lime-silica, and the great majority classify as natron glass on the basis of low K_2O and MgO concentrations (<1.5 wt%), while nine fragments classify as plant-ash glasses with relatively elevated K_2O and MgO concentrations (e.g. Lilyquist et al., 1993, Table 1). Sample results are presented in Tables A2–4, while Table 1 summarizes and outlines the main compositional characteristics of the natron groups recognized. Table 2 lists characteristics of the plant-ash glass groups. The nineteen natron type samples from the pilot paper on Geresa glass (Barfod et al., 2018) are not included in the tables and discussion of the present work. They are, however, included in Fig. 4c and d, demonstrating that they are fully consistent with the results of this larger study.

4.1. Natron glass

It has become clear that there were in the order of ten major primary glass production centres in the Levant and Egypt in the first millennium CE, each of which had a finite lifetime ranging from decades to several centuries. It has recently been shown that many of them may be distinguished on the basis of their major elements, particularly TiO_2, Al_2O_3, and SiO_2 contents (Foy et al., 2003; Schibille et al., 2017; Degryse, 2017; Freestone et al., 2018; Freestone, 2021). The low TiO_2 contents of the majority of the Jerash natron glass groups correspond with glass originating in the Levant, whereas relatively few belong to primary groups currently attributed to Egypt (Fig. 3).

Two samples with high TiO_2/Al_2O_3 and Al_2O_3/SiO_2 ratios correspond to the Egyptian group Série 2.1 (Fig. 3; Foy et al., 2003; equivalent to HLIMT of Ceglia et al., 2015). Their compositions exhibit the high Na_2O, MgO, MnO, and Fe_2O_3 characteristic of this group, for which production is generally dated to the sixth century (Table 1; Cholakova et al., 2015). A further group of four samples with high TiO_2/Al_2O_3 equate to the Egypt 1 category of Gratuze and Barrandon (1990) (Fig. 3), a type relatively uncommon outside Egypt. These samples are characterized by high titania, alumina, magnesia, and iron oxide contents (Table 1). Egypt 1 has been sub-divided and its chronology precisely determined by Schibille et al. (2019). Based on this, three samples from the NW Quarter correspond to Egypt 1b, a type produced between 720 and 780 CE (Fig. 3), but which must have dated before the abandonment of the city due to the earthquake of 749 CE. The fourth Egypt 1 sample, which falls into the Egypt 1a field in Fig. 3, does not fit strictly into any of the recognized Egypt 1 types due to its high CaO (above 6 wt%) combined with a relatively low Al_2O_3/SiO_2 ratio (Table 1; Fig. 3; Schibille et al., 2019). These features in combination with its high K_2O and P_2O_5 concentrations imply that this Egypt 1 type sample has experienced significant recycling (Table 1; see discussion).

Several samples with 0.4–0.7 wt% Sb_2O_5 but with Mn at background sand levels of c. 200 ppm (see Schibille et al., 2017) correspond to Roman Sb (Rom-Sb), as shown in Fig. 3 and Table 1. These show the relatively low Al_2O_3 and CaO, along with the high Na_2O, which are characteristic of Roman antimony-decolorised glass (Table 1). While it has been suspected for some time that the production of Roman Sb glass was located in Egypt (e.g. Degryse, 2014, 2017; Freestone, 2015; Jackson and Paynter, 2016; Gliozzo, 2017; Whitehouse, 2004), the evidence has been largely circumstantial. However, recent work using the isotopes of hafnium on a subset of the Gerasa samples in this study has confirmed their common origin with other groups generally accepted as having been made in Egypt, rather than from the Levant (Barfod et al., 2020). Note that major and trace elements for the samples analyzed for $^{176}Hf/^{177}Hf$, $^{87}Sr/^{86}Sr$ and $^{143}Nd/^{144}Nd$ ratios in Barfod et al. (2020) are presented in this study and marked with an asterix in column 3 of Table A2.

A second Sb-rich group contains both Mn and Sb above the sand background. The occurrence of both Sb and Mn in a natron glass which has not been opacified is generally taken as evidence of the mixing of Sb- and Mn-bearing glasses (e.g. Silvestri, 2008; Jackson and Paynter, 2016). The Gerasa data show a gap in Sb concentrations between 120 ppm and 800 ppm, and so for the purpose of the present paper the Roman SbMn group is defined as having >800 ppm Sb and >4000 ppm Mn (corresponding to above ~0.1 wt% Sb_2O_5 and 0.5 wt% MnO, respectively; Table 1; Tables A2–3).

The remaining natron glasses, representing the great majority of analyzed material, are Levantine (Fig. 3). Six of the Levantine-type sherds are strongly colored; they are therefore presented separately in Tables A2–3 and not included in the classification below due to the potential disturbances from the high concentrations of colorants (up to 31 wt% PbO, 12 wt% Fe_2O_3, and 3.6 wt% CuO; Tables A2–3).

The great majority of Levantine glasses analyzed typically have less than 50 ppm Sb (occasionally up to 120 ppm; Tables 1 and A2), suggesting minimal contamination by admixed Roman Sb glass. The dating

Table 1
Characteristics and mean compositions of natron glass groups and subgroups defined in this study.

Groups	Roman Sb	Roman–SbMn	High Mn – Low Al	Medium Mn – High Al	Low Mn (3 subgroups)			Foy 2.1	Egypt 1b	Egypt 1 recycled	Egypt 1b -High K_2O mix
Abbrev	Rom Sb	Rom SbMn	High Mn	Med Mn	High K_2O	Med K_2O	Low K_2O	Foy 2.1	Egypt 1b	Egypt 1 Re	–
Comment	*Pristine Roman Sb*	*Recycled Roman*	*Equivalent to Roman Mn*	*Recycled Jalame-type*	*Intensely recycled Apollonia-type*	*Recycled Apollonia-type*	*Mostly pristine Apollonia-type*	*Foy 2.1*	*Egypt 1b*	*Egypt 1-Apollonia Recycled*	*40% Egypt 60% Apo[c] calculated*
n	3	14	11	22	20	40	14	2	3	1	–
Origin	Egypt	Levant-Egypt mix	Levant	Levant	Levant	Levant	Levant	Egypt	Egypt	Levant-Egypt mix	Levant-Egypt mix
Likely date	1st–4th C	1st–4th C	1st–4th C	4–5th C	6–8th C	6–8th C	6–8th C	6th C	8th C	8th C	–
Screening criteria[a]	MnO <0.02 Sb_2O_5 >0.4	MnO >0.5 Sb_2O_5 >0.1	MnO >0.6 Sb_2O_5 <0.02 Al_2O_3 < 2.9	MnO 0.07–0.3 Sb_2O_5 <0.02 Al_2O_3 > 2.9	MnO <0.07 Sb_2O_5 <0.02 K_2O > 1	MnO <0.07 Sb_2O_5 <0.02 K_2O = 0.6–1	MnO <0.07[c] Sb_2O_5 <0.02 K_2O < 0.6	TiO_2 > 0.15 MgO >1 Fe_2O_3 > 1	TiO_2 > 0.5 CaO >3.5 Al_2O_3 > 4	TiO_2 = 0.28 CaO = 6.5 Al_2O_3 = 3.7	TiO_2 = 0.28 CaO = 7.1 Al_2O_3 = 3.5
SiO_2[b]	69.3	67.0	68.1	67.8	68.1	70.8	71.6	65.5	71.3	70.3	70.1
SD	(1.1)	(0.8)	(2.1)	(1.1)	(11.5)	(1.2)	(1.7)	(1.0)	(0.1)	(–)	
TiO_2[b]	0.08	0.09	0.07	0.09	0.10	0.08	0.08	0.17	0.54	0.28	0.28
SD	(0.01)	(0.01)	(0.02)	(0.01)	(0.01)	(0.01)	(0.01)	(0.01)	(0.02)	(–)	
NaO_2[b]	19.1	16.6	16.6	15.4	14.1	14.7	14.8	18.6	16.6	15.9	15.0
SD	(0.2)	(0.5)	(1.5)	(0.6)	(0.7)	(1.0)	(1.1)	(1.5)	(0.2)	(–)	
K_2O[b]	0.36	0.92	0.75	1.11	1.15	0.80	0.51	0.63	0.49	0.94	0.89
SD	(0.02)	(0.15)	(0.23)	(0.14)	(0.14)	(0.10)	(0.05)	(0.25)	(0.02)	(–)	
CaO[b]	6.02	8.82	8.25	9.97	9.82	8.36	7.73	7.27	2.94	6.54	7.09
SD	(0.92)	(0.74)	(1.27)	(0.81)	(0.77)	(0.74)	(0.78)	(1.37)	(0.15)	(–)	
Al_2O_3[b]	1.76	2.48	2.47	2.97	3.05	2.99	3.08	2.55	4.27	3.68	3.51
SD	(0.08)	(0.12)	(0.20)	(0.09)	(0.15)	(0.14)	(0.18)	(0.38)	(0.12)	(–)	
Fe_2O_3[b]	0.39	0.63	0.44	0.54	0.62	0.49	0.46	1.13	1.84	1.30	1.11
SD	(0.05)	(0.07)	(0.11)	(0.08)	(0.10)	(0.09)	(0.10)	(0.13)	(0.00)	(–)	
MgO[b]	0.62	0.72	0.62	0.73	0.76	0.64	0.62	1.26	1.01	0.89	0.86
SD	(0.19)	(0.04)	(0.12)	(0.06)	(0.12)	(0.07)	(0.08)	(0.25)	(0.02)	(–)	
MnO[b]	0.02	1.06	1.15	0.15	0.04	0.03	0.02	1.42	0.04	0.08	0.04
SD	(0.00)	(0.73)	(0.75)	(0.06)	(0.01)	(0.01)	(0.00)	(0.43)	(0.01)	(–)	
P_2O_5[b]	0.04	0.20	0.14	0.18	0.25	0.13	0.07	0.13	0.09	0.22	0.18
SD	(0.00)	(0.05)	(0.05)	(0.05)	(0.05)	(0.03)	(0.01)	(0.07)	(0.01)	(–)	
Cl[b]	1.26	0.78	0.87	0.70	0.73	0.85	0.92	0.99	0.95	0.78	0.81
SD	(0.04)	(0.12)	(0.14)	(0.14)	(0.10)	(0.09)	(0.11)	(0.25)	(0.02)	(–)	
V[b]	8.57	27.2	17.7	10.9	12.3	10.2	8.89	33.1	45.7	28.6	26.1
SD	(1.09)	(14.9)	(7.8)	(1.5)	(1.3)	(1.4)	(1.35)	(1.6)	(1.0)	(–)	
Co[b]	1.16	9.28	8.33	3.67	4.34	1.86	1.53	9.58	5.97	4.08	4.96
SD	(0.07)	(7.97)	(5.85)	(1.25)	(2.44)	(0.46)	(0.40)	(2.53)	(0.07)	(–)	
Cu[b]	12.6	51.2	62.6	167	88.2	33.7	7.73	75.8	5.03	169	54.8
SD	(1.9)	(15.6)	(80.4)	(52)	(111.8)	(83.5)	(6.10)	(16.6)	(0.15)	(–)	
Rb[b]	4.64	8.35	9.85	13.0	13.1	10.5	8.13	6.29	8.39	13.2	11.2
SD	(0.57)	(0.72)	(2.63)	(0.8)	(2.8)	(1.3)	(0.92)	(2.60)	(0.26)	(–)	
Sr[b]	466	525	513	497	467	460	446	681	221	337	372
SD	(68)	(91)	(50)	(25)	(39)	(35)	(49)	(206)	(9)	(–)	
Zr[b]	44.9	48.7	41.0	45.2	51.5	46.7	46.1	94.8	192	116	110
SD	(1.7)	(3.8)	(5.0)	(2.9)	(3.3)	(5.3)	(4.5)	(9.1)	(9)	(–)	
Sn[b]	0.30	18.0	2.91	9.09	7.37	2.40	0.59	3.95	0.43	9.85	4.59
SD	(0.06)	(8.3)	(4.21)	(3.77)	(9.37)	(4.01)	(0.48)	(0.26)	(0.02)	(–)	
Sb[b]	4516	1887	23.6	22.1	2.79	1.09	0.21	416	0.16	0.54	1.75
SD	(1009)	(756)	(37.1)	(0.02)	(2.13)	(1.09)	(0.20)	(143)	(0.04)	(–)	
											250

(*continued on next page*)

Table 1 (*continued*)

Groups	Roman Sb	Roman-SbMn	High Mn – Low Al	Medium Mn – High Al	Low Mn (3 subgroups)			Foy 2.1	Egypt 1b	Egypt 1 recycled	Egypt 1b -High K_2O mix
Abbrev	Rom Sb	Rom SbMn	High Mn	Med Mn	High K_2O	Med K_2O	Low K_2O	Foy 2.1	Egypt 1b	Egypt 1 Re	–
Ba[b]	136	331	430	279	259	253	257	295	239	281	
SD	(11)	(86)	(157)	(17)	(21)	(14)	(13)	(4)	(5)	(–)	
La[b]	5.64	6.92	6.73	6.86	7.26	6.73	6.67	8.47	9.52	8.83	8.20
SD	(0.43)	(0.67)	(0.46)	(0.33)	(0.46)	(0.39)	(0.43)	(0.40)	(0.23)	(–)	
Nd[b]	5.71	6.83	6.73	7.05	7.30	6.90	6.88	8.27	10.3	9.24	8.56
SD	(0.45)	(0.57)	(0.47)	(0.31)	(0.41)	(0.37)	(0.48)	(0.34)	(0.3)	(–)	
Yb[b]	0.52	0.65	0.65	0.66	0.69	0.65	0.64	0.79	1.11	0.93	0.88
SD	(0.03)	(0.07)	(0.05)	(0.03)	(0.05)	(0.04)	(0.05)	(0.02)	(0.05)	(–)	
Pb[b]	24.3	186.5	80.0	228	79.4	28.1	12.5	86.6	5.51	67	50
SD	(2.3)	(85)	(139)	(104)	(67.1)	(27.3)	(16.4)	(52.4)	(0.91)	(–)	

Abbreviations: Abbrev = Abbreviations; n = number of samples.

[a] MnO, Al_2O_3, K_2O, TiO_2 and CaO in wt% (Table A2) and Sb_2O_5 in wt% (Table A3). Screening criteria are guides for some groups, e.g. High Mn group is defined as cluster in Fig. 4a.

[b] Concentrations of major element oxides and Cl in wt% (Table A2) and trace elements in ppm (Table A3). Numbers in parenthesis correspond to 1 std dev.

[c] Theoretical mix calculated by mixing 60% mean values for recycled Apollonia type subgroup (High K_2O; column 6) with 40% mean values for Egypt 1b (column 10).

of Levantine glass on the basis of its composition and, thus, its assignment to specific primary furnaces are not straightforward. However, this is required if we are to isolate groups that are likely to represent contemporaneous material. At the present time, three main primary production centers have been identified in the Levant for the period of interest: (1) Jalame, near Haifa, which appears to have ceased production in the 4th century CE (Weinberg 1988; excavations by the Israel Antiquities Authority in 2015 have confirmed primary tank furnaces, see Ben Zion 2016); (2) Apollonia-Arsuf, which operated in the 6th–7th centuries CE (Tal et al., 2004; Freestone, 2020); and (3) Bet Eli'ezer, Hadera (Gorin-Rosen, 1995; Freestone et al., 2000) from which the glass products appear to date to the 8th century CE (Phelps et al., 2016). There are uncertainties around the 5th century CE as primary furnaces have not been securely identified for this period, but compositional continuity suggests that furnaces in the Apollonia region may have been supplying raw glass at that time (Freestone, 2020); the data of Phelps et al. *op. cit.* suggest that Apollonia production continued in the 8th century CE.

The use of beach sands in the glass-making furnaces of the eastern Mediterranean coastal plain leads to substantial overlaps in their compositions; previous attempts to discriminate between their products were based upon bi-plots of CaO versus Al_2O_3 (Freestone et al., 2000) and more recently taking into consideration Na_2O and SiO_2 but overlaps are still apparent (Al Bashaireh et al., 2016; Phelps et al., 2016; Barfod et al., 2018). Here we have subdivided the Levantine glass according to MnO, Al_2O_3 and Sb (Fig. 4a and b; Table 1). MnO-decolorised glass was common in the first to third centuries and manganese is present in some raw chunks of the fourth century (Brill, 1988); however, there is no evidence for the addition of MnO to raw glass at Apollonia (Freestone, 2020), and it does not seem to have been added as a decoloriser to Levantine glass after the 5th century (Schibille et al., 2017, following Foy et al., 2003). In addition, Al_2O_3 contents are higher in Apollonia and Bet Eli'ezer glass products than in Mn-decolorised glass of the 1–4th centuries (e.g. Freestone, 2020) and are also high in the glass from Jalame (Brill, 1988). The Gerasa data show breaks around 2.7 wt% Al_2O_3 and at around 0.07 wt% MnO, allowing a relatively clear cut subdivision of the Levantine glass as shown in Fig. 4a:

(1) High Mn (High Mn – Low Al), corresponding to earlier Roman Mn (Rom-Mn) production of first–third centuries; this group has relatively low Al_2O_3 (<2.9 wt%) combined with high MnO (>0.6 wt%) and up to 120 ppm Sb (Table 1; Fig. 4b). Group members can have MnO as low as 0.1 wt%, but this is consistent with the Roman Mn category (e.g. Jackson and Paynter, 2016, Fig. 4a and b; Table A2). This group overlaps with the Roman SbMn group in Fig. 4a.

(2) Low Mn (Low Mn – High Al), with MnO <0.07 wt% combined with Al_2O_3 > 2.7 wt%, and assigned to Apollonia production (sixth–eighth centuries); this group has Sb below 10 ppm and frequently below 1 ppm (Table A3; Table 1; Fig. 4b). Given that the natural concentration of MnO in Levantine sand is 0.02–0.03 wt%, some of these samples contain traces of Mn from recycling although Sb concentrations below 1 ppm indicate minimal contamination by Roman glass. This group, the most abundant analyzed, is further subdivided below into 3 subgroups on the basis of K_2O (Table 1; see discussion).

(3) Med Mn (Medium Mn – High Al), which shows both early and late characteristics. Sb is consistently above background, ranging from 2 to 60 ppm (Tables A3). The intermediate MnO combined with high Al_2O_3 (Fig. 4a; Table 1) suggest that this group is later than Rom-Mn, perhaps corresponding to the fourth century Jalame production and possibly production into the fifth century. Fig. 4b shows the very strong control on Mn and Sb in these samples from end-member compositions with low and high SbMn, respectively. (*Med Mn* group in Fig. 4b; $R^2 = 0.84$). This could be explained by very small amounts (note log scale in

Table 2
Mean values (±1 std dev) for the plant-ash-type glasses from Northwest Quarter.

Group name	*PA-1* – O, P, Q (n = 6)	*PA-2* – K (n = 2)	*PA-3* - K (n = 1) Bracelet
Type	Mesopotamia Type 1	Mesopotamia Type 2	Eastern Mediterranean
K_2O – wt%	2.5 ± 0.2	2.4 ± 0.5	3.6
Al_2O_3 – wt%	2.9 ± 0.7	1.5 ± 0.2	1.5
MgO – wt%	4.5 ± 0.5	7.2 ± 0.6	3.8
Fe_2O_3 – wt%	1.6 ± 0.5	0.5 ± 0.1	0.5
Zr – ppm	64 ± 19	35 ± 1	145
Li – ppm	14 ± 1 (51[a])	32 ± 1	12
Cr – ppm	102 ± 29 (642[a])	53 ± 25	11
MgO/CaO	0.6 ± 0.1	1.2 ± 0.3	0.5
$^{86}Sr/^{87}Sr$	0.70848 ± 16	0.70839 ± 2	–
ε_{Nd}	−6.0 ± 0.4	−5.5 ± 0.7	–
ε_{Hf}	−13.7 ± 1.0 (−6.3[a])	−11.3 ± 1.8	–

[a] Values for PA-1 outlier in Figs. 6 and 7 (see Tables A2 and A4 for details).

Fig. 4b) of Roman SbMn-type glasses mixing with pristine Jalame-type glass (see discussion).

Fig. 4c and d show how the glass samples from the earlier study of glass from the Northwest Quarter (Barfod et al., 2018) conform to the groupings outlined above.

The source attributions of the Gerasa Levantine groups are consistent with and supported by the previous approach using the ratios CaO/Al_2O_3 and Na_2O/SiO_2 (Fig. 5). The majority of the *Low Mn* group map onto the Apollonia field, while both the *High Mn* and *Med Mn* groups map onto Jalame/Rom-Mn, which occupy the same space in the figure. This is fully consistent with the interpretation that they correspond to 1st–4th century Rom-Mn and Jalame-type glasses, respectively. Note also in Fig. 5 the high Na_2O/SiO_2 ratio of the Roman-Sb group, which is of Egyptian origin and was produced close to the Egyptian natron sources (cf. Freestone, 2021). The position of the Rom-SbMn glasses between Rom-Mn and Rom-Sb is consistent with the view that SbMn is a mixture of Levantine and Egyptian glass (Fig. 5).

It is not possible to confidently assign each individual sample to Roman Mn (1–4th century), Jalame (4th century) or Apollonia/Byzantine (6–7th century) types with confidence, as there are gaps in the available evidence around the fourth to sixth centuries, and compositional overlaps between categories remain. However, there is a recognizable relationship between composition and probable date, and this suggests that the groupings are reasonably robust. These conclusions are consistent with the typological dating of the glass, which although it

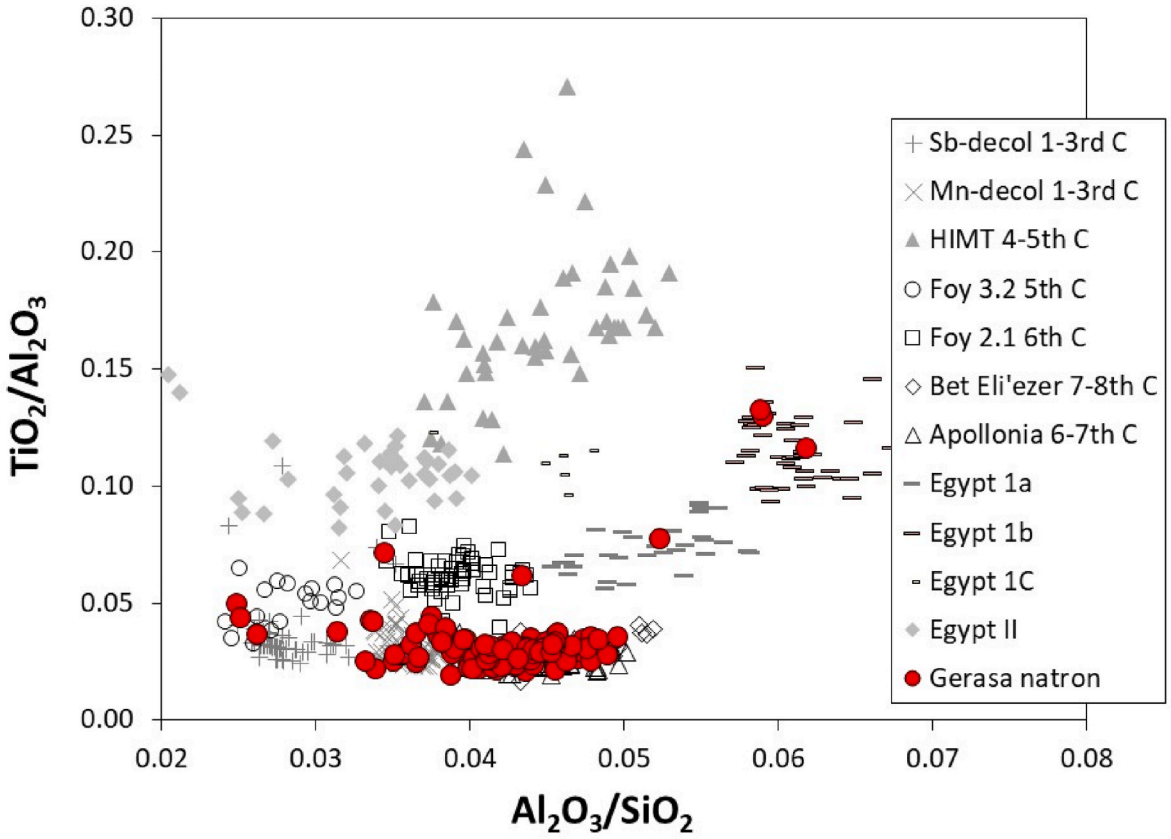

Fig. 3. TiO_2/Al_2O_3 versus Al_2O_3/SiO_2 ratios for natron glass from NW Quarter in Gerasa (red circles) compared to main primary production groups of the first millennium CE from the Levant (Mn-decolorised, Apollonia and Bet Eli'ezer) and Egypt (Sb-decolorised, HIMT, Foy 3.2 & 2.1, Egypt 1a, b & c and Egypt II). Base data from Foy et al. (2003), Silvestri (2008), Silvestri et al. (2008), Schibille et al. (2019) and Freestone et al. (2015). This shows the majority of the natron glass in the Northwest Quarter of Gerasa to originate from the Levantine coast. (For interpretation of the references to color in this figure legend, the reader is referred to the Web version of this article.)

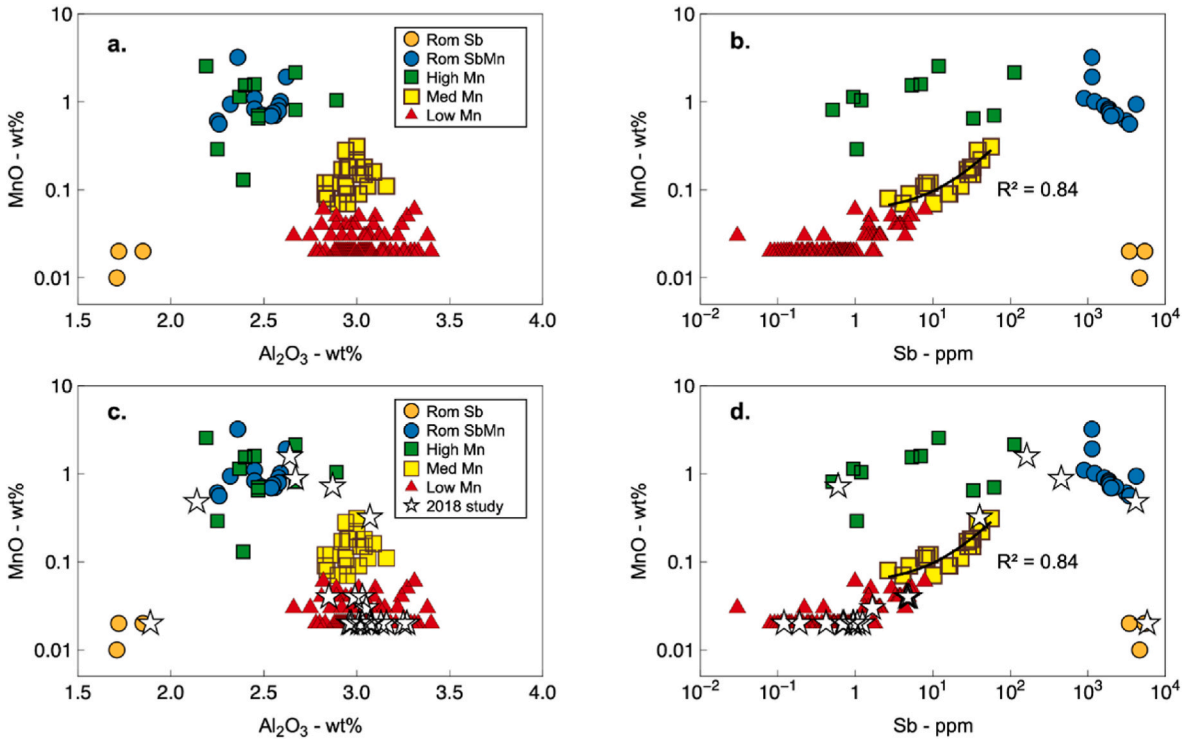

Fig. 4. MnO [wt%] (note log scale) versus a. Al_2O_3 [wt%] and b. Sb [ppm] (note log scale) concentrations for Levantine natron-type glass from Geresa, showing the division into the three major compositional groups; *High Mn*, *Med Mn* and *Low Mn* groups. Roman antimony decolorised glass (Rom-Sb) and Roman SbMn (Rom-SbMn) groups are shown for comparison. c. Log MnO [wt%] versus a. Al_2O_3 [wt%] and d. Log Sb [ppm] for Levantine natron-type glass groups in this study compared to samples from the same area from Barfod et al. (2018).

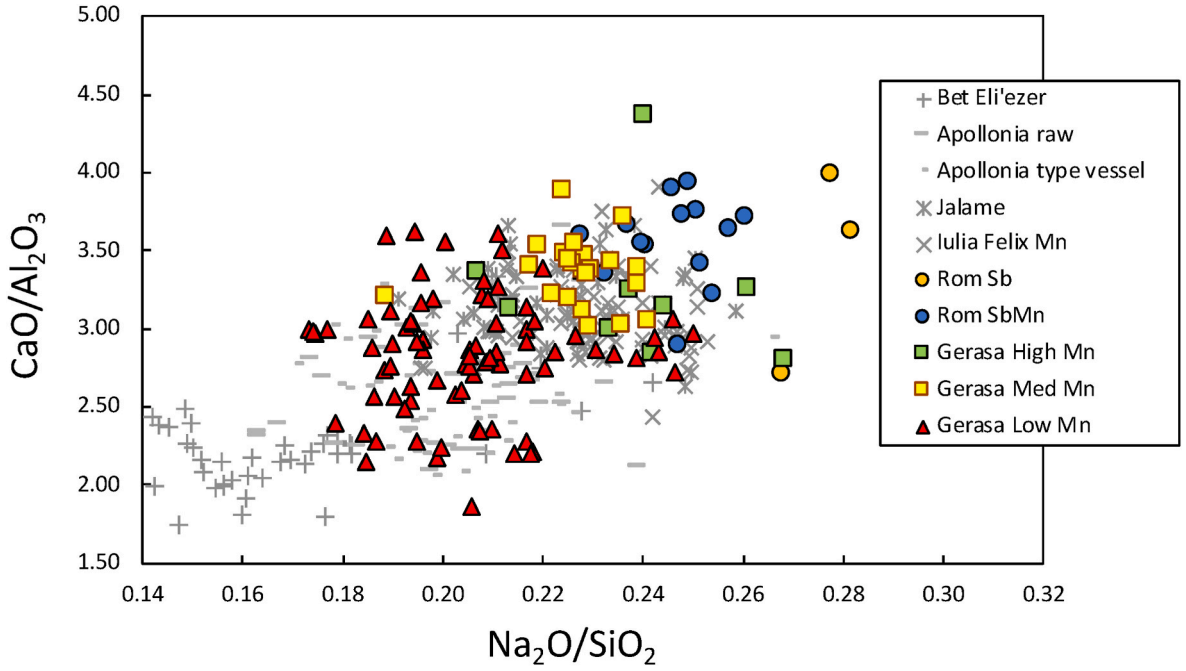

Fig. 5. Comparison of CaO/Al_2O_3 and Na_2O/SiO_2 ratios in natron glass with Levantine characteristics compared with primary production types. Base data from Brill (1988), Silvestri et al. (2008), Tal et al. (2004), Freestone et al. (2000, 2008), Phelps et al. (2016) and unpublished data for Bet Eli'ezer. Gerasa *High Mn* and *Med-Mn* groups map on to Iulia Felix and Jalame glass of 1st–4th centuries, whereas Gerasa *Low Mn* group maps onto Apollonia.

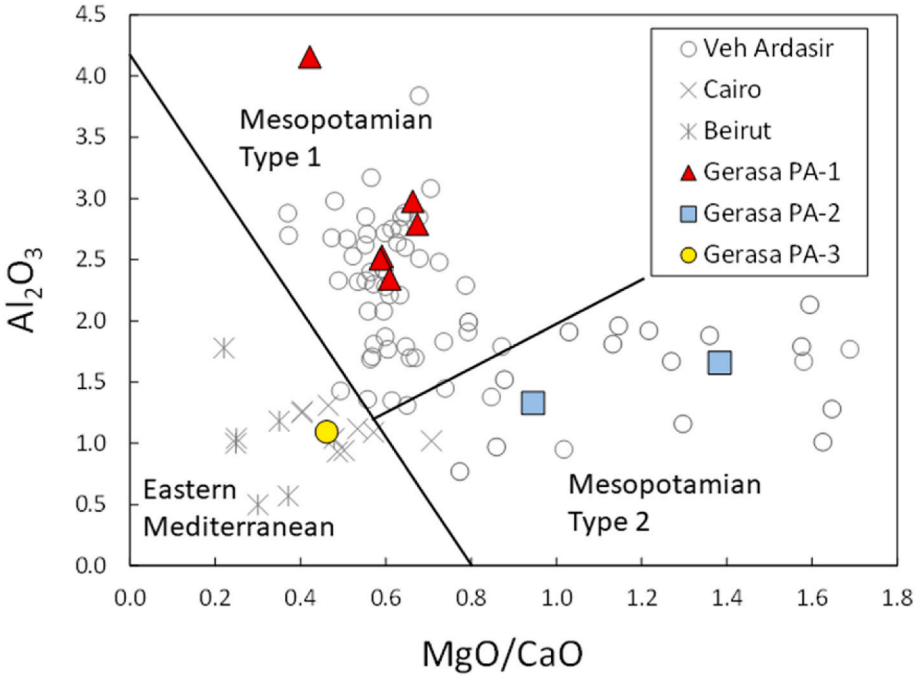

Fig. 6. Al_2O_3 [wt%] versus MgO/CaO ratio for plant-ash glass from Gerasa compared with plant-ash glass from Cairo and Beirut (Henderson et al., 2016) and Sasanian glass from Veh Ardasir (Mirti et al., 2008, 2009). Base plot and boundaries after Phelps (2018).

cannot be precise, provides some useful indications. As observed from Tables A2, vessels dated Roman (as opposed to Byzantine or Islamic) are almost entirely restricted to compositional groups Roman Sb, Roman SbMn, Roman Mn (*High Mn*), and Jalame-type (*Med Mn)*, while the characteristic vessels in the Apollonia (*Low Mn)* group are almost entirely Byzantine or early Islamic in form. It is emphasized that because the groups identified show significant evidence for recycling, which is context sensitive (see below) the precise subdivisions used here, based upon Al, Mn and Sb, are unlikely to be universal, but correspond to the specific context of the NW Quarter of Gerasa.

4.2. Plant-ash glass

Nine samples have the high MgO and K_2O contents characteristic of soda plant ash. The samples fall into three groups, divided on the basis of Al_2O_3 contents into: *PA-1* with >2.5 wt% Al_2O_3 (includes four sherds from House of the Tesserae in Trench P and two other sherds from Trenches O and Q), *PA-2* with c. 1.5 wt% Al_2O_3 (two sherds from House of the Scroll in Trench K), and *PA-3*, which comprises a single sherd with 1.09 wt% Al_2O_3 from House of the Scroll (Table 2). The major element compositions of *PA-1* and *PA-2* correspond to the broad Mesopotamian Types 1 and 2 of Phelps (2018), as shown in his discrimination diagram (Fig. 6). The single example of *PA-3* (J14-Kg-3-188) falls in the "Eastern Mediterranean" field, and corresponds quite closely to glass from Cairo analyzed by Henderson et al. (2016) (Figs. 6–7). However, this is a black bracelet, as opposed to the other samples, which are vessel fragments. The composition of this bracelet corresponds well to the only other plant-ash glass material identified in Geresa, namely two glass beads recovered from the same context 3 in trench K (see section 2.1; Barfod and Søgaard, forthcoming; Bobou and Krag, forthcoming). Thus, it is interesting that so far *PA-3*-type plant-ash glass includes only items of personal adornment.

Henderson et al. (2016) have observed that Cr and Li concentrations tend to be lower in Syrian and Egyptian glasses relative to those produced in Mesopotamia. Fig. 7 compares the plant-ash glasses from Gerasa with those from a range of sites analyzed by Henderson et al. (op. cit.); glass from Nishapur (Iran) and Raqqa, Syria (which appears to lie in several compositional groups) has been neglected in the plot to enhance its readability. The majority of the Gerasa *PA-1* and *PA-2* glasses plot in the high Li and Cr region characteristic of central Mesopotamian glass, as characterized by analyses from Samarra and Ctesiphon, but there is a single outlier which has very high Li and Cr concentrations. *PA-3* (the single black bangle) is, as suggested by its major element composition (Fig. 6), related to an eastern Mediterranean production (Fig. 7).

Three samples from *PA-1* Group and two samples from *PA-2* Group were analyzed for Sr, Nd and Hf isotopes (Tables 2 and A4). The relatively low and consistent Sr isotope compositions (0.7083–0.7084) combined with ε_{Nd} isotopic compositions around −6.0 observed for *PA-1* and *PA-2* Groups compare well to observations for Sassanian glasses at Veh Ardasir (adjacent to Ctesiphon) in present-day Iraq, where

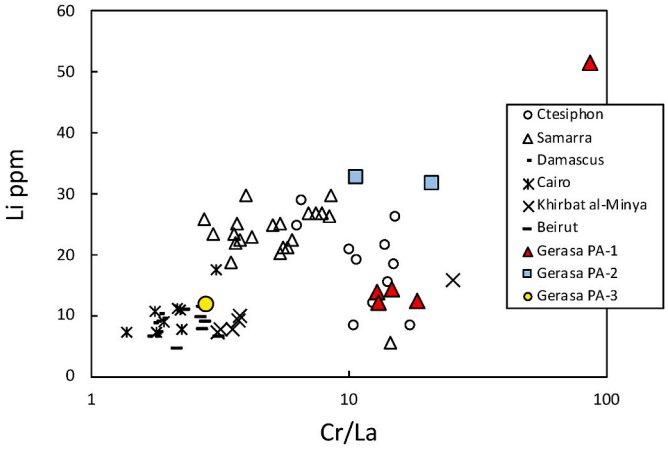

Fig. 7. Comparison of Li [ppm] versus Cr/La ratios for Gerasa plant-ash glass with glass from Mesopotamia (unfilled symbols: Ctesphon, Samarra), the Levant (single line black symbols: Damascus, Beirut, Khirbat al-Minya) and Egypt (Cairo), comparative data from Henderson et al. (2016). The Gerasa vessels (*PA-1* and *PA-2* Groups) are Mesopotamian, while the bracelet (*PA-3*) appears Egyptian or Syrian. Note log scale of Cr/La.

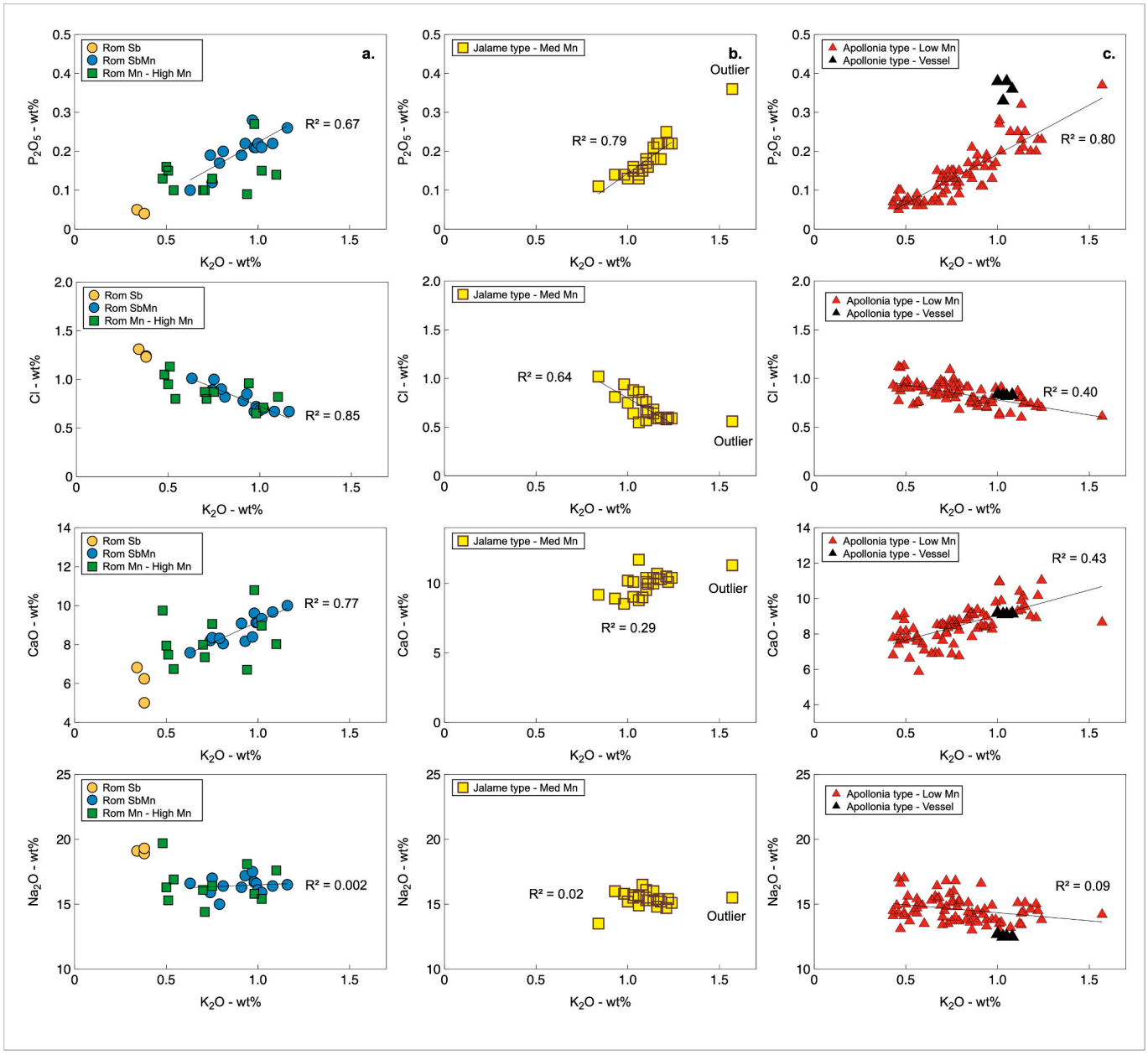

Fig. 8. Variations of P_2O_5 (top row) Cl (middle upper row), CaO (middle lower row) and Na_2O (lower row) versus K_2O [reported in wt%] for a) Rom-Sb, Rom-SbMn, and *High Mn* (Rom-Mn), b) *Med Mn*, and c) *Low Mn* glass groups from the Northwest Quarter. Note that four samples from a single vessel are presented separately as black triangles due to their high P_2O_5.

comparable ranges are reported for both Mesopotamian-type 1 and 2 samples (Mirti et al., 2009; Ganio et al., 2013 in their Fig. 3) and are also consistent with the Sr and Nd isotopic ratios of Mesopotamian glass of the Late Bronze Age (Degryse et al., 2015). Thus, despite the limited isotope data available, the correspondence in Nd and Sr systematics observed for the plant-ash glass from the NW Quarter are consistent with the elemental data, suggesting a Mesopotamian origin for these vessel glasses. Hafnium isotope analysis, the first reported for plant-ash glass, shows lower ε_{Hf} values of −12.6 to −14.9 for *PA-1* relative to −9.6 to −12.1 for *PA-2* Groups, indicating minor differences in the zircon mineral assemblages within the glass-making sands for the two groups (Tables A4; Table 1). The outlier of Group *PA-1*, J15-Pe-16-196, has the highest observed ε_{Hf} of −6.8 for any ancient glass so far analyzed (Tables A4; Table 2), suggesting that this glass originates elsewhere, possibly further east and indicating the potential of Hf for source discrimination.

5. Discussion

5.1. Recycling intensity

For the purpose of the discussion of recycling, we consider the (non-exotic/Levantine) natron glass in the four main groups identified above; Rom-SbMn type, Rom-Mn type (*High Mn*), Jalame-type (*Med Mn*), and Apollonia-type (*Low Mn*).

It is conventional to consider recycling in terms of those colorant-related elements (transition metals) which are unintentionally incorporated in the batch during repeated episodes of re-melting (e.g. Mirti et al., 2001; Silvestri et al., 2008; Paynter and Jackson, 2016; Rehren and Freestone, 2015; Sainsbury, 2018). However, while these components can provide a robust indication that recycling has occurred, their concentrations depend upon the amount of colored glass added to the batch, which itself is dependent upon context (e.g. Duckworth, 2020).

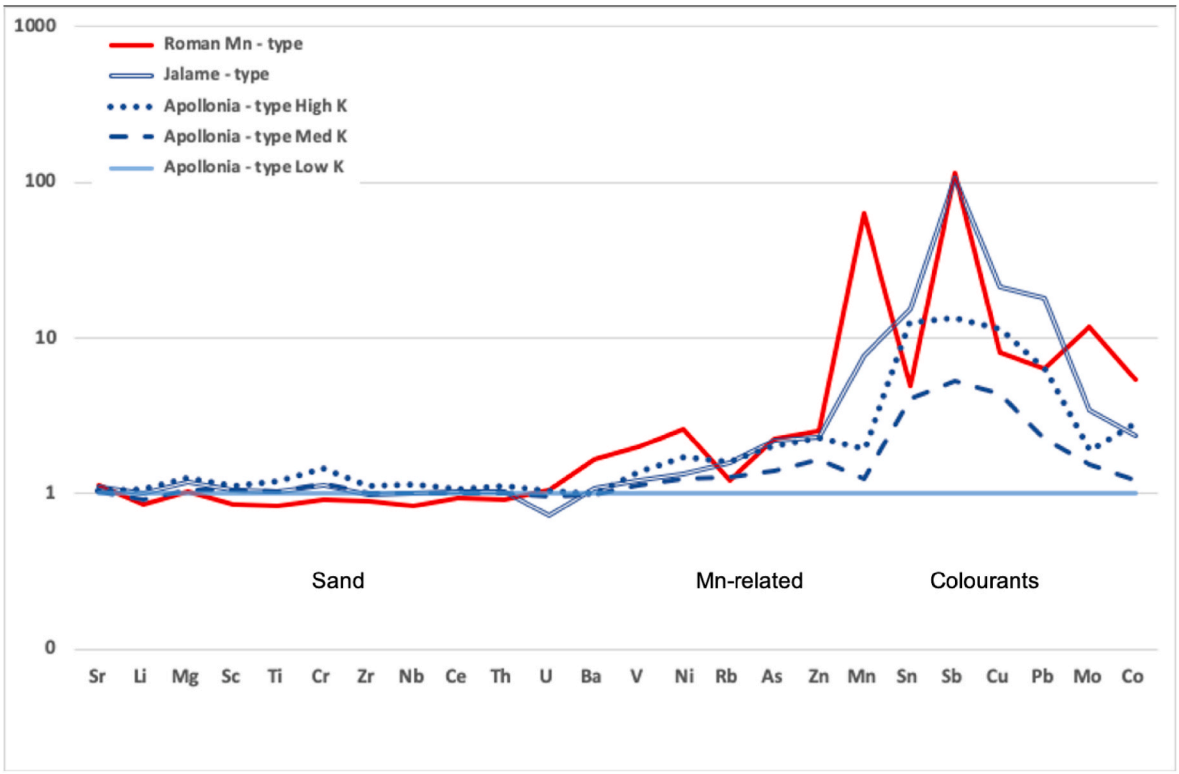

Fig. 9. Mean values for trace elements (note log scale) from Gerasa natron glass groups and subgroups normalized to Apollonia-type *Low K_2O* subgroup illustrating how repeated remelting (≈elevated K) leads to elevated elements introduced from glass containing de-colorants, colorants, and/or opacifiers during secondary glass-working (right side), whereas concentrations of elements originating from the raw materials used in primary glass production remain relatively constant (left side).

For example, the incorporation of glass from mosaics can have a major effect (Schibille and Freestone, 2014; Barfod et al., 2018). The amount of colored glass may therefore not be a reliable indicator of the *intensity* of recycling, where recycling intensity is an integral of the total number of recycling events that have contributed to a batch of glass and the contribution of each event to the bulk composition. If the dependence of the glass economy upon recycling processes is to be understood, then a measure of intensity is required.

If it is assumed that to a first approximation each recycling event involves re-melting glass cullet to approximately the same temperature for the same period of time, then the cumulative amount of time that the glass contributing to a batch has been at high temperature provides an indication of recycling intensity. Components reflecting the amount of time at high temperature include enhanced K_2O and P_2O_5 concentrations which represent contamination of the glass by fuel ash vapour (e.g. Tal et al., 2008; Rehren et al., 2010; Schibille et al., 2017; for experimental demonstration see Paynter, 2008); in the Levant this effect is likely to have been enhanced by the use of potash-rich fuel such as olive pomace (Barfod et al., 2018). As shown in the top row of Fig. 8 there are strong correlations between K_2O and P_2O_5 in the Gerasa natron glass groups, indicating that contamination of this type was common. A concomitant depletion in Cl due to vaporization (see also Freestone and Stapleton, 2015; Al-Bashaireh et al., 2016, Barfod et al., 2018) is also apparent, particularly in the Roman SbMn (middle row in Fig. 8). Similarly, CaO increases with K_2O and P_2O_5 (lower row in Fig. 8; see also Al-Bashaireh et al., op. cit.), and while this may relate to contamination with particulate fuel ash in Roman SbMn glass ($R^2 = 0.77$), recent work suggests that during Byzantine times it may be due to the use of a lime lining in Byzantine furnaces in the Levant (Chen et al., 2021). This latter mechanism would explain the higher degree of decoupling for K_2O and CaO reflected by lower correlation coefficients ($R^2 = 0.40$ and 0.43) observed for Jalame-type and Apollonia-type groups relative to Roman SbMn glass ($R^2 = 0.77$; Fig. 8). The implication of this would be that recycling practices and/or furnace configurations and melting practices changed from Roman to Byzantine times in the city. It also suggests that CaO is likely to be a less reliable indicator of recycling intensity than K_2O, P_2O_5, and Cl. The degree of contamination by CaO will have depended upon additional factors such as the thickness of the lime lining in the furnace tank, the effectiveness with which it was applied, and the care taken by the glass workers to separate waste furnace glass from the lime release agent before it was remelted. It will therefore have a less direct relationship with the duration of melting than the other compositional changes.

It has been suggested that significant soda loss may occur during glass reheating as observed in modern glass production, (Freestone 2015), which might be expected to result in a highly viscous glass, limiting the number of times glass recycling is possible. We have investigated the possible loss of sodium from the Gerasa glass but the evidence is weak. Fig. 8 (lower row) demonstrates that the Na_2O contents of the Roman and Byzantine glasses do not show a strong negative correlation with K_2O, as might be expected if sodium was evaporated from the glass. Lukas (2021) has pointed out that melting conditions in ancient furnaces were very different from those in modern glass melting where soda loss is observed, notably in temperatures which in modern furnaces are at least two hundred degrees higher, with longer melting durations and clean, oxidizing atmospheres, and these factors are likely to explain the difference in behavior. While we would not rule out the possibility of sodium loss during melting of all ancient glass – the occurrence of soda-rich glazes on the superstructure of furnaces (Chen et al., 2021) suggests that some sodium evaporation does occur – on the basis of the present evidence, this does not appear to be to a degree which would, for example, affect compositional classification.

Although a direct relationship between the concentrations of transition metal colorants and the intensity of recycling is not necessarily expected, weak positive correlations between K_2O and transition metal colorants and decolorizers such as Co, Sb, and Cu may be observed

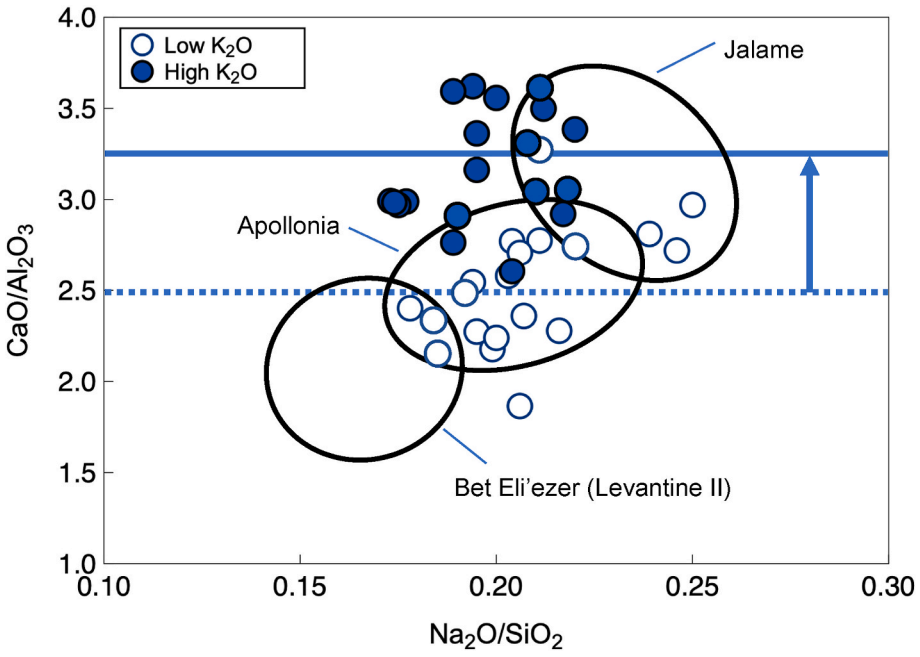

Fig. 10. CaO/Al_2O_3 versus Na_2O/SiO_2 ratios for Low K_2O (0.4-0.6 wt%) and High K_2O (1.0-1.2 wt%) Apollonia-type subgroups compared with the compositional fields of primary glasses from factories at Jalame, Apollonia, and Bet Eli'ezer (black ellipses – note that these are only approximate representations; see Fig. 5 for true extents). The horizontal solid blue line shows the mean value for High K_2O glass (=intensely recycled) and the punctuated blue line for the relatively pristine Low-K_2O glass. The effect of extensive recycling is thus enhanced CaO contents of the glass, shifting it out of the Apollonia field. (For interpretation of the references to color in this figure legend, the reader is referred to the Web version of this article.)

within the Gerasa groups. To interrogate this effect, we have further subdivided the Apollonia-type (*Low-Mn*) group into 3 subgroups on the basis of their K_2O concentrations; *Low K_2O* with $K_2O < 0.6$ wt%, *Med K_2O* with K_2O between 0.6 and 1.0 wt%, and *High K_2O* with $K_2O > 1.0$ wt %; Tables 1 and A2), assuming that the potash contents are a reflection of the intensity of recycling which each glass has undergone (Table 1). The *Low K_2O* sub-group is considered to have been least recycled; in fact, the Sb content of glass in this sub-group is consistently below 1 ppm, equivalent to glass from the primary furnaces at Apollonia (Fig. 4b; Brems et al., 2018) so it is considered to represent pristine Levantine primary glass. Fig. 9 compares the trace element compositions of the most abundant natron glass groups by normalizing their averages to the average values of the *Low K_2O* subgroup (Table 1, Table A3). Those elements expected to have been derived primarily from the glass-making sand (e.g. Ti, Zr, Sr and Mg) are shown on the left of the diagram, while those associated with colorants, decolorants, and opacifiers (e.g. Cu, Co, Pb, Sn, Mn and Sb) are on the right (Fig. 9). The profiles of the sand-related elements on the left are relatively flat and close to unity, implying that the sand was essentially the same for all groups (i.e. Levantine coastal sand). Variations around the elements Ba, V, Ni in the groups richer in MnO reflect their presence in the manganese oxide used to decolorize the glass, as noted elsewhere for Ba (Cosyns et al., 2018; Paynter, 2006). Leaving these aside, it is clear that for the Apollonia-type glasses, increasing potash is correlated to an increase in all of the colorant elements, with the *High K_2O* glasses having higher concentrations than the *Med K_2O* subgroup glasses. However, the concentrations of the colorant elements in the earlier Roman Mn and Jalame-type glasses are higher than in the later Apollonia-type groups, even higher than in the Apollonia *High K_2O* subgroup which, on the basis of its approximately equivalent contents of K, P, Ca oxides, and Cl

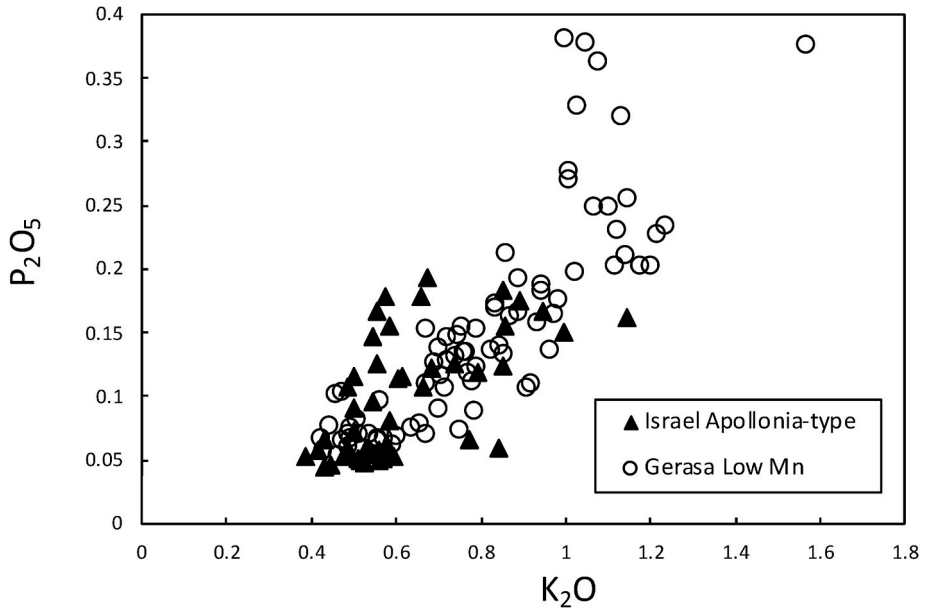

Fig. 11. K_2O and P_2O_5 in Apollonia-type glass from Gerasa NW Quarter, compared with vessels from Israel analyzed by Phelps et al. (2016).

(Fig. 8; Table 1), would appear to have undergone an equivalent intensity of recycling. It was previously observed (Barfod et al., 2018) that the concentration of colorants in recycled glass would depend on the reservoir of colored glass available for recycling. In the present case, the higher colorant elements in the Roman Mn and Jalame-type glasses are likely to reflect the well-known phenomenon that higher amounts of colored glass were in circulation in the earlier Roman periods. Interestingly, pristine Roman Sb glass with no evident signs of recycling has survived (Fig. 8); reflecting the care taken to conserve this high-quality colorless glass (Jackson, 2005; Freestone 2015; Gliozzo, 2017).

Contamination that is decoupled from K_2O is evident by strong correlations between Fe and Ti, V, Nb ($R^2 \sim 0.6–0.8$; Suppl. Fig 1) observed for the SbMn Roman, Jalame-type (Med Mn) and Apollonia-type (Low Mn) glass. For the subset of Jerash glass studied in Barfod et al. (2018), we ascribed such correlations to differences in the minor mineral assemblages of the glass-making sands given the concurrent correlation between Mg and Fe. However, the lack of Fe–Mg correlation in this study ($R^2 = 0.2$; Suppl. Fig 1) implies that this observation was an artifact of the small samples size in our previous study. Also, the overall increase in Fe with increasing degree of recycling (as reflected by an increase in K) confirms the strong link between the Fe–Ti–V–Nb correlations and recycling (Suppl. Fig 2). Incorporation of high Fe and Ti-rich HIMT or Foy 2.1 glass in the recycling process can be excluded as an explanation for the correlations given that 1. it would require unrealistically high volumes and 2. these glass types are high in Mn and Mg, which would then be expected to increase with Fe as well. Instead, contamination from recycling furnace or crucible ceramics, fly-ash or colored glass are plausible explanations (e.g. Schibille et al., 2016). It has also been observed that lime-rich furnace linings may contribute significant Fe-contamination (Chen et al., 2021).

In summary, while we see strong evidence of recycling in the NW Quarter, there are observable differences in the recycling effects recorded by chronologically older relative to younger glass, illustrating the higher availability of colored and decolorised glass during and immediately following the Roman period.

5.2. The effect of recycling intensity on source attribution

Significant compositional changes due to recycling have been identified above for a range of components. These potentially interfere with source assignation. CaO content, which has been used to discriminate between Levantine groups (and also Egypt 2; Freestone et al., 2000) can be misleading in this respect. Individual analyses may differ substantially from the core grouping and require careful evaluation. Thus, the composition of glass from primary furnaces at Apollonia averages between 8.1–8.6% CaO (Freestone, 2020), but the mean CaO of glass from our High K_2O "Apollonia-type" group is 9.85%, while the maximum CaO content is 11%, well above the range of the primary production site (Tables 1 and A2). Similarly, the mean CaO content of glass from the production site of Jalame is 8.7% (data of Brill, 1988), while our inferred "recycled Jalame" group, Med Mn has mean CaO of 10% with a maximum of 11.3% (Tables 1 and A2).

Given that we interpret the High K_2O subgroup as recycled and Low K_2O as pristine members of the Apollonia-type group, these should all plot within or close to the Apollonia field in Fig. 10 if unaffected by recycling. However, the location of most High K_2O samples above the Apollonia field and into the Jalame field illustrates how the effect of recycling is indicated to have resulted in a mean increase of around 0.7 for the CaO/Al_2O_3 ratio (blue arrow in Fig. 10), while the Na_2O/SiO_2 ratio appears unaffected. Classification of Late Roman and Byzantine Levantine glass using CaO/Al_2O_3 ratios should therefore be limited to samples with K_2O contents below 0.6 wt% if it is to be robust.

For similar reasons, attempts to match vessel glass to primary production assemblages using multivariate statistical techniques on unfiltered compositional assemblages are likely to be challenging. Approaches based upon categorization using simple algorithms (e.g. Brems and Degryse, 2014) are more likely to be successful.

5.3. Recycling at Gerasa in context

Recycling was a significant practice at Gerasa, and the majority of the glass assemblage have experienced some recycling and/or have been subjected to prolonged periods of re-melting. Using the concept of recycling intensity, which is based upon those changes in composition related to the duration of melting rather than on the materials available to be recycled, we are now in a position to make comparisons between glass assemblages and the extent to which glass was being recycled. In this sense the recycling intensity is considered to be a qualitative indicator of the average total number of melting cycles per unit of glass. In principle, it should be possible to use experimental data for compositional change, such as those of Paynter (2008) to calibrate the archaeometric data to produce a more quantitative index of glass recycling, related to the actual duration of melting, but this is not prudent with the available experimental data. Secondary glass furnaces in the Roman and Byzantine Levant were frequently based upon tanks (Gorin-Rosen 2000), rather than the pots (crucibles) used in the case study of Paynter (op.cit.), and the degree of contamination/evaporation would have been strongly dependent upon the surface area of glass exposed to the furnace atmosphere and its ratio to the volume of glass, which were very different. The configuration of the furnace and the nature of the fuel would also have been important. Similar experiments using various volumes of glass and with different wood fuels are needed to evaluate these effects, and for these reasons we restrict ourselves to a qualitative interpretation.

Fig. 11 compares potash and phosphorus oxide contents of the Apollonia-type (Low Mn) glass from Gerasa with vessels in Apollonia-type glass from a number of sites in modern Israel (mainly Jerusalem, Sepphoris and Tiberias), using data of Phelps et al. (2016). A substantial proportion of the Gerasa glass assemblage is significantly more contaminated than the Israel glasses, as illustrated by the higher K_2O and P_2O_5.

Indeed, of the 86 Apollonia-type glass sherds from the NW Quarter, only 20 (23%) have less than 0.6 wt% K_2O and are close to pristine, compared to 64% of the 50 Israel samples (including 78% of 27 glasses from Jerusalem). These findings suggest that the intensity of recycling (i.e. the average total number of cycles per unit of glass,) was significantly greater in Gerasa. This view is supported by the negative correlation between potash and chlorine for the Gerasa glass which appears to represent a progressive loss of volatile Cl with prolonged heating, a correlation not observed for the sites closer to the coast, again suggesting a less intense recycling regime. Thus, although Jerash is situated in the Levant and is less than 150 km from the glass production sites at Apollonia as the crow flies, it appears to have been particularly dependent on glass recycling to meet the needs of the population. This is consistent with the findings at other sites in Jordan which exhibit high K_2O in Apollonia-type glass (e.g. Petra, Rehren et al., 2010; Umm el-Jimal, Al-Bashaireh et al., 2016).

The possibility that different degrees of potash enrichment were due to differences in furnaces or fuels opposite sides of the Jordan Valley cannot be dismissed. However, analysis of material from a Late Byzantine workshop at Ramla, between Tel Aviv and Jerusalem, shows very high enrichment in potash (all analyzed vessel fragments have > 0.9 wt % K_2O; Tal et al., 2008), demonstrating that similar contamination could occur in furnaces nearer the coast. Evidence of potash contamination is also seen in vessels associated with secondary production at Apollonia itself (Freestone et al., 2008). It is therefore more likely that the difference in K_2O and P_2O_5 contents of Gerasa and the material from cities in Israel reflects a different intensity of recycling, and that the glass industry in Gerasa was more dependent upon recycled cullet than was the case for major settlements west of the Jordan Valley. The high degree of recycling is likely to have been a result of a strong general demand for products due to the prosperity of the city. However, the

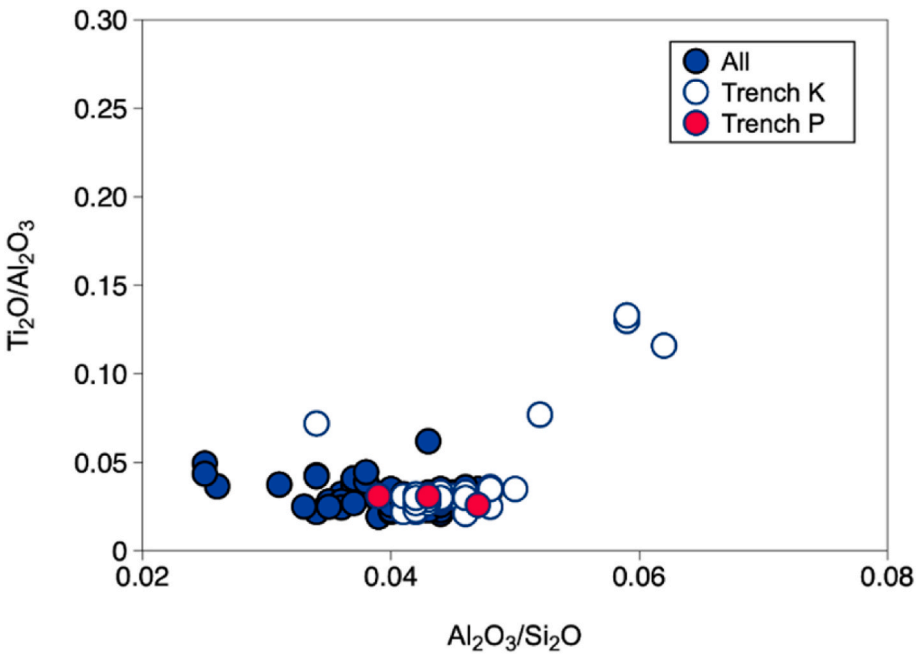

Fig. 12. TiO_2/Al_2O_3 versus Al_2O_3/SiO_2 for natron glass from the House of the Scroll in trench K (open circles) and the House of the Tesserae (red circles) projected onto all NW Quarter glass (blue circles; also see Fig. 3) showing that glass types from the two houses are post-Roman and include Jalame/Apollonia types, characterized by relatively high Al_2O_3 as well as Egyptian glass types Foy 2.1 and Egypt 1. (For interpretation of the references to color in this figure legend, the reader is referred to the Web version of this article.)

balance between fresh primary glass and the recycling of cullet is likely to reflect the geographical situation.

Numerous finds of raw glass off the Palestinian coast (Galili et al., 2015) reflect the proximity to the sea of the major primary glass production sites of the Roman through the Early Islamic period and the importance of marine transport in glass distribution. Overland transport of raw glass from West to East is likely to have been more expensive than movement along the coast, rendering fresh glass less accessible. Evidence of recycling is therefore much more apparent at inland sites such as Gerasa, Petra, and Umm el-Jimal. This is consistent with the evidence from ceramic assemblages in the region, which indicate a major difference between the presence of imports in sites near the coast, relative to those inland (Bes et al., 2020). The apparent higher dependency of settlements to the east of the Jordan Valley on recycling of old materials would have been facilitated by the strong local exchange systems which were in operation at this time (Walmsley, 2012). Even so, the presence of exotic glass indicates that recycling should not be understood as a symptom of less connectivity or broken networks to the coastal regions. Rather, since other areas of Gerasa's urban economy, such as its active pottery production, show a strong local production to meet the local demand and only very few imports, it seems that Gerasa was able to rely on an optimized circular economy and was able to operate with a low influx of external resources (Bes et al. *op. cit.)*.

5.4. Exotic glass from the Houses of the Scroll and Tesserae

Much of the glass recovered and analyzed in the present study is likely to have been discarded material which, although available, had not been collected for recycling. It represents a range of contexts from Roman through to Early Islamic. However, this is not the situation for the material from the House of the Scroll (in Trench K) and the House of the Tesserae (in Trench P) where activity was truncated by the earthquake of 749 CE. Here, we can expect that a higher proportion of glass was in use towards the very end of the life of the city. Of the exotic glass, one of two examples of Foy 2.1, all four examples of Egypt 1 as well as two examples of plant-ash glass vessels of type PA-2 and the bracelet of type PA-3 were recovered from the House of the Scroll. Furthermore, two glass beads of type PA-3 (Barfod and Søgaard, forthcoming) and three gold-gilded tesserae of Foy 2.1 (Boschetti et al., 2021) have also been reported from this house. From the House of the Tesserae, four sherds of the plant-ash-type 1 (PA-1) were recovered. Combined, this amounts to twelve of the fifteen post-Roman objects with exotic compositions analyzed in this study (Figs. 3 and 6).

The four Egypt 1 samples from the House of the Scroll are compositionally dated to the eighth century and, furthermore, the plant-ash glasses from both houses are typologically Early Islamic. With the exception of the sample corresponding to Foy 2.1 (generally accepted to be a 6th-century type, e.g. Cholakova et al., 2015; Maltoni et al., 2016; Schibille et al., 2017), this is thus consistent with use at the time of the earthquake. It seems likely that these exotic glass compositions are particularly well-represented in the House of the Scroll and the House of the Tesserae because they were in use at the very end of the occupation and therefore were not used as cullet for recycling and re-melted. If the exotic glasses from the two Umayyad houses had been intensely recycled, their chemical signatures would have been highly diluted by the large mass of Levantine glass, and eventually lost. This process is observed for the only other Foy 2.1 in this study found away from the houses (in Trench O) given that this shows evidence of recycling (K_2O = 0.8 wt%, P_2O_5 = 0.17 wt%; Table A2). Furthermore, one of the Egypt 1 samples (J14-Kh-51-3; Tables A2-A3) stands out due to its relatively high CaO (above 6 wt%) and low Al_2O_3/SiO_2 ratio (Table 1; Fig. 3; Schibille et al., 2019) combined with its high K_2O and P_2O_5 concentrations, implying significant recycling. Mixing calculations show that the major, trace, and isotopic composition of this sample can be explained by mixing 'pristine' Egypt 1b (represented by the Egypt 1b samples found in the same context) with highly recycled (High K_2O) Apollonia-type glass in the proportions 1:1.5. The theoretical mix is listed and compared to the observed recycled Egypt 1b in Table 1 and Tables A2-A4 and show significant overlap. Interestingly, the mixture of Egypt 1b and High K_2O Apollonia glass has yielded a composition which, in Fig. 3, appears to lie in the field of Egypt 1a. It may be envisaged that a batch of Egyptian 1b glass was procured to be blown into vessels and that, as this was depleted, Apollonia-type cullet was added to the tank or pot to allow blowing to continue. A wreck of a ship carrying both Egypt 1 and Apollonia-type cullet has recently been reported off the coast of Israel (Natan et al., 2021).

The interpretation that exotic glass from the House of the Scroll and the House of the Tesserae most likely would have been absent from the archaeological record due to recycling had it not been for the truncation of activity on the site due to the earthquake is supported by the analyses

of Apollonia-type (Low Mn) glass in the two assemblages. Fig. 12 shows that the Levantine natron glass recovered from the houses is Late, with high Al_2O_3/SiO_2 ratios, and that Roman material is absent here. Of 76 Apollonia-type (Low Mn) vessels analyzed from the whole Gerasa assemblage, 20 (26%) are in the pristine Low-K_2O subgroup, which shows minimal evidence of recycling. In contrast, 10 of 20 analyzed vessels (50%) from the two houses belong to the Low K_2O subgroup, confirming that glass from this context has a higher representation of fresh/unrecycled glass than the NW Quarter of Gerasa as a whole.

The glasses from contexts K and P have typologies that date to the Late Byzantine to Early Islamic periods and include types well known at the site (a twisted dark bracelet and mainly bottles with in-folded rims and applied trail decoration), which implies that they were made in the region from imported raw glass or cullet, rather than having been traded over long distances in their final form. Without the evidence of production debris of an appropriate composition, production in or around Jerash itself would be difficult to prove but if it is indeed the case, trade in Egyptian and perhaps even Mesopotamian raw glass in the Early Islamic period and perhaps before would be implied.

The apparent absence of glass made in the primary furnaces at Bet Eli'ezer, Hadera, from the assemblage and in particular from the Umayyad Houses is unexpected; the Bet Eli'ezer furnaces are considered to have been operative in the Umayyad period (Phelps et al., 2016), while the vessels of Egypt 1 composition clearly indicate that the House of the Scroll assemblage has a significant component of Umayyad-period glass. It is not clear why Bet Eli'ezer glass should not have reached Gerasa in significant quantities before the middle of the 8th century, and it may be that the dating of the Bet Eli'ezer output is in need of closer attention.

The presence of an unexpectedly high proportion of glass types which are not associated with primary production on the Levantine coast is likely to reflect in part the decline of Levantine production known to have occurred in the Early Islamic period and its substitution by imported glass from the south and the east (Freestone et al., 2015; Phelps et al., 2016). Egyptian natron-based glass is not common in analyzed assemblages from the northern Levant at this time although it has been detected in Israel, with Egypt 1a used for window glass and tesserae at the Umayyad residential site of Khirbar al-Minya (Adlington et al., 2020) and occasionally for vessels elsewhere (Phelps et al., 2016). Egypt 2 becomes widely distributed in the Abbasid period but this type postdates the Jerash assemblage (Schibille et al., 2019). In Jordan, analyses of several Egyptian glasses have been reported from the South (Rehren et al., 2010) but not from the North (Al-Bashaireh et al., 2016; Arinat et al., 2014; El-Khouri, 2014). Foy 2.1 has so far only been reported as (in particular gold-leaf) tesserae (Adlington et al., 2020; Boschetti et al., 2021), although chunks of this type have been observed from off-shore deposits, presumably lost from ships during transport (Freestone and Gorin-Rosen, work in progress). Plant-ash glass made on the Levantine coast appears in the late eighth century in Israel, but Mesopotamian vessels appear first in the Abassid period (Phelps 2018). The Mesopotamian compositions identified here therefore represent early examples of the movement of glass from the East as natron glass production declines. The occurrence of these exotic types at Gerasa is therefore of considerable interest; they are clearly a record of significant long-distance trade, either in raw glass or finished glass objects.

6. Conclusions

This paper reports an unusually detailed analytical programme undertaken upon a glass vessel assemblage recovered from the excavation of a limited area of the ancient city of Gerasa and has allowed a number of conclusions to be made which contribute to both the understanding of the site and assemblage as well as to the interpretation of glass compositional data in general. From a methodological perspective, we have developed further previous approaches to discrimination allowing a complex diachronic dataset of Roman to Byzantine Levantine glass to be sub-divided and attributed individual production centers using major and minor elements. We have also developed the concept of the relative *intensity* of glass recycling, which is essentially a reflection of the cumulative number of re-melting events which have contributed to a batch of glass. It is based upon the concentrations of volatile elements such as K, P, and Cl and their relationship to melting duration, and is regarded as a more reliable indicator of the intensity of recycling than the relative admixture of a second glass type (such as opaque and/or colored glass, Roman-Sb etc). This is because any position on the mixing line between the end-member compositions (revealed for example by the content of colorant elements) could be the result of one or many recycling episodes and is not necessarily diagnostic. Calcium oxide concentrations were also enhanced during the recycling process, and we observe that care should be taken to use glass with relatively low K_2O, when using CaO/Al_2O_3 ratios to classify Levantine glass from the Late Roman and Byzantine periods as glass with low K_2O is less likely to have been intensely recycled. In principle, the concept of recycling intensity that we have developed should be applicable to other glass assemblages. However, the extent to which the specific indicators of recycling intensity used here may be applied beyond the eastern Mediterranean is unclear, because the potential uses of K-rich olive pomace as a fuel here (e.g. Gorin-Rosen, 2000; Barfod et al., 2018), and of lime as a release agent in furnaces (Chen et al., 2021), are likely to have enhanced the compositional effects observed. Preliminary observations suggest however that K, P, and Cl show qualitatively similar variations in natron glass from other regions, and we advocate further exploration of their variation.

Although the dominant Levantine glass was all made from similar coastal sands, it is possible to distinguish several chronological groups from the Roman to the Umayyad periods, based largely upon alumina, manganese oxide, and soda concentrations, and attribute these to the major primary productions close to the Mediterranean coast. Given the evidence for intensive recycling across the whole period, it is significant that these glass groupings remain distinctive and have not blurred. This reflects the fact that there was a constant loss of material from the system, so that some discarded glass was not retrieved to be recycled. Our sample (and presumably glass within archaeological contexts in general) is thus largely composed of this glass which escaped the cycle of re-melting. Over time, lost glass was replenished by fresh material until its compositional signature was diluted beyond recognition in the material in use at a particular time. Even so, the presence of antimony at above background levels in several samples of Apollonia-type glass from Umayyad contexts K and P hints at a continuity of recycling where traces of Roman material are still present in the reservoir of recycled material several centuries later.

Exotic glass from Egypt and Mesopotamia was recovered, especially from the House of the Scroll in Trench K and the House of the Tesserae in Trench P, where activity was truncated by the earthquake of 749 CE. While the presence of plant-ash glass reflects the accelerating decline of Levantine natron production in the eighth century, these closed contexts favored a more representative preservation of the glass that was actually in use. It therefore seems probable that some evidence of exotic glass from earlier periods has been lost due to the intensity of recycling activities.

Comparison of the composition of Apollonia-type glass at Gerasa with that from sites West of the River Jordan suggests that recycling was particularly intensive, although the city had access to fresh raw glass from the tank furnaces close to the Mediterranean coast. This intense recycling reflects the high demand for glass in the urban environment of Gerasa coupled with the higher cost of overland transport as opposed to coastal trade. Hence, while the exotic materials indicate connectivity over long distances, local trading networks were dominant.

Declaration of competing interest

The authors declare no competing interests.

Acknowledgements

The Danish-German Jerash Northwest Quarter Project was co-directed by Achim Lichtenberger and Rubina Raja between 2011 and 2017. The work of the project and the following analysis were supported by the Carlsberg Foundation (RR), the Danish National Research Foundation under Grant DNRF119 (Centre of Excellence, Centre for Urban Network Evolutions – UrbNet) (RR), the Danish National Research Foundation under Grant 26-123/8 (Niels Bohr Professorship in Geoscience) (CEL), the Deutsche Forschungsgemeinschaft (AL); Deutscher Palästina-Verein (AL); the EliteForsk initiative of the Danish Ministry of Higher Education and Science (RR), and H. P. Hjerl Hansens Mindefondet for Dansk Palæstina-forskning (RR). We thank O. Neill (GeoAnalytical Lab, Washington State University) for performing the EMP analyses, R. Andreasen for assistance during isotope analysis and E.J. Rosenberg and I. Søgaard for assistance during sample preparation and ICP-MS analyses. Discussions with P. Ebeling as well as insightful reviews by Th. Rehren and an anonymous reviewer significantly improved this paper.

Appendix A. Supplementary data

Supplementary data to this article can be found online at https://doi.org/10.1016/j.jas.2022.105546.

References

Adlington, L.W., Ritter, M., Schibille, N., 2020. Production and provenance of architectural glass from the Umayyad period. PLoS One 15, e0239732.
Al-Bashaireh, K., 2016. Production technology of glass bracelets from the west cemetery of Umm el-Jimal in Northeastern Jordan. Mediterranean Archaeology & Archaeometry 16.
Al-Bashaireh, K., Al-Mustafa, S., Freestone, I.C., Al-Housan, A.Q., 2016. Composition of Byzantine glasses from Umm el-Jimal, northeast Jordan: insights into glass origins and recycling. J. Cult. Herit. 21, 809–818.
Arinat, M., Shiyyab, A., Abd-Allah, R., 2014. Byzantine glass mosaics excavated from the Cross Church, Jerash, Jordan: an archaeometrical investigation. Mediterranean Archaeol. Archaeometry 14, 43–53.
Baldoni, D., 2019. Archaeological evidence for craft activities in the area of the sanctuary of Artemis at Gerasa between the Byzantine and Umayyad periods. In: Lichtenberger, A., Raja, R. (Eds.), Byzantine and Umayyad Jerash Reconsidered: Transitions, Transformations, Continuities. Jerash Papers 4. Turnout, Brepols, pp. 115–158.
Barfod, G.H., Freestone, I.C., Lesher, C.E., Lichtenberger, A., Raja, R., 2020. 'Alexandrian'glass confirmed by hafnium isotopes. Sci. Rep. 10, 1–7.
Barfod, G.H., Freestone, I.C., Lichtenberger, A., Raja, R., Schwarzer, H., 2018. Geochemistry of Byzantine and early Islamic glass from Jerash, Jordan: typology, recycling and provenance. Geoarchaeology 33, 623–640.
Barfod, G.H., Søgaard, I., forthcoming. Compositions and raw materials of jewellery from the Northwest Quarter. In: Lichtenberger, A., Raja, R. (Eds.), Small Finds. Final Publications from the Danish-German Jerash Northwest Quarter Project V, Jerash Papers 10 (Turnout: Brepols).
Baur, P.V.C., 1938. Glassware. In: Kraeling, C.H. (Ed.), Gerasa, City of the Decapolis: an Account Embodying the Record of a Joint Excavation Conducted by Yale University and the British School of Archaeology in Jerusalem (1928–1930), and Yale University and the American Schools of Oriental Research. American Schools of Oriental Research, New Haven, pp. 505–546.
Ben Zion, I., 11 April 2016. Ancient Glass Kilns Clear View into Industry's Even Older History. Times of Israel available at:, 2016. https://www.timesofisrael.com/israels-oldest-glass-kilns-point-to-ancient-silicon-valley/.
Bes, P., Brughmans, T., Lichtenberger, A., Raja, R., Romanowska, I.A., 2020. Ceramics in cities in context: an overview of published roman imperial to Umayyad pottery in the southern levant. In: Lichtenberger, A., Raja, R. (Eds.), Hellenistic and Roman Gerasa. The Archaeology and History of a Decapolis City. Jerash Papers 5. Brepols: Turnout, pp. 55–118.
Bidegaray, A.I., Cosyns, P., Gratuze, B., Terryn, H., Godet, S., Nys, K., Ceglia, A., 2019. On the making, mixing and trading of glass from the Roman military fort at Oudenburg (Belgium). Archaeol. Anthrop. Sci. 11, 2385–2405.
Bobou, O., Krag, S., Forthcoming. The jewellery from The northwest Quarter. In: Lichtenberger, A., Raja, R. (Eds.), Small Finds. Final Publications from the Danish-German Jerash Northwest Quarter Project V, Jerash Papers 10 (Turnout: Brepols).
Boschetti, C., Lichtenberger, A., Raja, R., Wootton, W., Schibille, N., 2021. Loose Glass Tesserae and Lost Decorations: Chronology and Production of Mosaics from Gerasa's Northwest Quarter. Archaeometry.
Boschetti, C. & W. T. Wootton (in press). "Mosaic glass tesserae from The northwest Quarter of Jerash", in: A. Lichtenberger & R. Raja (eds), Architectural Elements and Finds, Mosaics, and Wall-Paintings. Final Publications from the Danish-German Jerash Northwest Quarter Project IV, Jerash Papers 9 (Turnhout: Brepols).
Boyer, D.D., 2018. The role of landscape in the occupational history of Gerasa and its hinterland. In: Lichtenberger, A., Raja, R. (Eds.), The Archaeology and History of Jerash: 100 Years of Ecavations. Brepols Publishers, pp. 59–86.
Brems, D., Degryse, P., 2014. Trace element analysis in provenancing Roman glass-making. Archaeometry 56, 116–136.
Brems, D., Freestone, I.C., Gorin-Rosen, Y., Scott, R., Devulder, V., Vanhaecke, F., Degryse, P., 2018. Characterisation of Byzantine and early Islamic primary tank furnace glass. J. Arch. Sci. Rep. 20, 722–735.
Brill, R.H., 1988. Scientific investigations of the Jalame glass and related finds. In: Excavations at Jalame: Site of a Glass Factory in Late Roman Palestine, pp. 257–294.
Ceglia, A., Cosyns, P., Nys, K., Terryn, H., Thienpont, H., Meulebroeck, W., 2015. Late antique glass distribution and consumption in Cyprus: a chemical study. J. Archaeol. Sci. 61, 213–222.
Chen, C., Freestone, I.C., Gorin-Rosen, Y., Quinn, P.S., 2021. A glass workshop in 'Aqir, Israel and a new type of compositional contamination. J. Arch. Sci. Rep. 35, 102786.
Cholakova, A., Rehren, T., Freestone, I.C., 2015. Compositional identification of 6th c. AD glass from the Lower Danube. J. Archaeol. Sci. Rep. 7, 625–632.
Cosyns, P., Oikonomou, A., Ceglia, A., Michaelides, D., 2018. Late Hellenistic and early Roman slumped and cast glass vessels from the House of Orpheus at Paphos, Cyprus. An interim report. J. Archaeol. Sci. Rep. 22, 524–539.
Degryse, P., 2014. Glass Making in the Greco-Roman World: Results of the ARCHGLASS Project. Leuven University Press.
Degryse, P., 2017. Chemical signature and scale of production of primary glass factories around the Mediterranean in the first millennium AD. Annales du 20e Congres de l'Association Internationale pour l'Histoire du Verre. Romont 175-180.
Degryse, P., Lobo, L., Shortland, A., Vanhaecke, F., Blomme, A., Painter, J., Gimeno, D., Eremin, K., Greene, J., Kirk, S., Walton, M., 2015. Isotopic investigation into the raw materials of Late Bronze Age glass making. J. Archaeol. Sci. 62, 153–160.
Donovan, J.J., Snyder, D.A., Rivers, M.L., 1993. An improved interference correction for trace element analysis. Microbeam Anal. 2, 23–28.
Donovan, J.J., Tingle, T.N., 1996. An improved mean atomic number correction for quantitative microanalysis. J. Microsc-Oxford 2, 1–7.
Duckworth, C.N., 2020. Seeking the invisible: new approaches to roman glass recycling. In: Duckworth, C.N., Wilson, A. (Eds.), Recycling and Reuse in the Roman Economy. Oxford University Press, pp. 301–356.
Duckworth, C.N., Cuénod, A., Mattingly, D.J., 2015. Non-destructive μ-XRF analysis of glass and metal objects from sites in the Libyan pre-desert and Fazzan. Libyan Stud. 46, 15–34.
El-Khouri, L., 2014. Glass production in the early Byzantine period (4th–7th century) at Gadara (Umm Qais), Jordan, area W, 2011 season of excavation. Levant 46, 89–97.
Foy, D., Picon, M., Vichy, M., Thirion-Merle, V., 2003. Caracterisation des verres de la fin de l'Antiquité en Mediterranée occidentale: L'emergence de nouveaux courants commerciaux. In: Foy, D., Nenna, M.-D. (Eds.), Echanges et commerce du verre dans le monde antique: Actes du Colloque de l'Association Francaise pour l'Archeologie du Verre, Aix-en-Provence et Marseille, 7–9 juin 2001, 41–86. Editions Monique Mergoil, Montagnac.
Freestone, I.C., 2015. The recycling and reuse of Roman glass: analytical approaches. J. Glass Stud. 57, 29–40.
Freestone, I.C., 2020. Apollonia glass and its markets: an analytical perspective. In: Tal, O. (Ed.), Apollonia-Arsuf. Final Report of the Excavations, Volume II. Excavations outside the Medieval Town Walls. Institute of Archaeology, Tel Aviv University.
Freestone, I.C., 2021. Glass production in the first millennium CE: a compositional perspective. In: Klimscha, F. (Ed.), Ancient Glass and Glass Production. Berlin Studies of the Ancient World 67. TOPOI.
Freestone, I.C., Degryse, P., Lankton, J., Gratuze, B., Schneider, J., 2018. HIMT, glass composition and commodity branding in the primary glass industry. In: Rosenow, D., Phelps, M., Meek, A., Freestone, I.C. (Eds.), Things that Travelled: Glass in the First Millennium CE. UCL Press, London, pp. 159–190.
Freestone, I.C., Gorin-Rosen, Y., Hughes, M.J., 2000. Primary glass from Israel and the production of glass in late antiquity and the early Islamic period. MOM Éditions 33, 65–83.
Freestone, I.C., Jackson-Tal, R.E., Tal, O., Taxel, I., 2015. Glass production at an early Islamic workshop in Tel Aviv. J. Archaeol. Sci. 62, 45–54.
Freestone, I.C., Jackson-Tal, R.E., Tal, O., 2008. Raw glass and the production of glass vessels at late Byzantine Apollonia-Arsuf, Israel. J. Glass Stud. 50, 67–80.
Freestone, I.C., Stapleton, C.P., 2015. Composition Technology and Production of Coloured Glasses from Roman Mosaic Vessels. Oxbow.
Galili, E., Gorin-Rosen, Y., Rosen, B., 2015. Mediterranean coasts, cargoes of raw glass. Hadashot Arkheologiyot – Excav. Surv. Israel 127, 1–15.
Ganio, M., Gulmini, M., Latruwe, K., Vanhaecke, F., Degryse, P., 2013. Sasanian glass from Veh Ardašīr investigated by strontium and neodymium isotopic analysis. J. Arch. Sci. 40, 4264–4270.
Ganio, M., Boyen, S., Fenn, T., Scott, R., Vanhoutte, S., Gimeno, D., Degryse, P., 2012a. Roman glass across the Empire: an elemental and isotopic characterization. Anal. Atomic Spectr. 27, 743–753.
Ganio, M., Boyen, S., Brems, D., Scott, R., Foy, D., Latruwe, K., Molin, G., Silvestri, A., Vanhaecke, F., Degryse, P., 2012b. Trade routes across the Mediterranean: a Sr/Nd

isotopic investigation on Roman colourless glass. Glass Technol. Eur. J. Glass Sci. Technol. 53, 217–224.
Gliozzo, E., 2017. The composition of colourless glass: a review. Archaeol. Anthrop. Sci. 9, 455–483.
Gorin-Rosen, Y., 1995. Hadera, Bet Eli'ezer. Excav. Surv. Israel 13, 42–43.
Gorin-Rosen, Y., 2000. The ancient glass industry in Israel: summary of the finds and new discoveries. In: Nenna, M.-D. (Ed.), La Route du verre. Ateliers primaires et secondaires du second millenaire av. J.-C. au Moyen Age. Lyon: Maison de l'Orient et de la Mediterranee Jean Pouilloux, vol. 33. MOM Éditions, pp. 49–63.
Gratuze, B., Barrandon, J.N., 1990. Islamic glass weights and stamps: analysis using nuclear techniques. Archaeometry 46, 439–468.
Henderson, J., Chenery, S., Faber, E., Kröger, J., 2016. The use of electron probe microanalysis and laser ablation-inductively coupled plasma-mass spectrometry for the investigation of 8th–14th century plant ash glasses from the Middle East. Microchem. J. 128, 134–152.
Jackson, C.M., 2005. Making colourless glass in the Roman period. Archaeometry 47, 763–780.
Jackson, C.M., Paynter, S., 2016. A great big melting pot: exploring patterns of glass supply, consumption and recycling in Roman Coppergate. York. Archaeometry 58, 68–95.
Jackson-Tal, R.E., 2021. The glass finds from The northwest Quarter of Jerash. In: Lichtenberger, A., Raja, R. (Eds.), Glass, Lamps and Jerash Bowls. Final Publications from the the Danish-German Jerash Northwest Quarter Project III. Jerash Papers 8. Brepols, Turnout, pp. 13–49.
Kalaitzoglou, G., Lichtenberger, A., Raja, R., 2015. Preliminary report of the fourth season of the Danish-German Jerash Northwest Quarter project 2014. Annu. Dep. Antiq. Jordan 59, 11–43.
Kennedy, D., 2007. Gerasa in the Decapolis: A "Virtual Island" in Northwest Jordan. Duckworth, London.
Kraeling, C.H., 1938. Gerasa, City of the Decapolis: an Account Embodying the Record of a Joint Excavation Conducted by Yale University and the British School of Archaeology in Jerusalem (1928–1930), and Yale University and the American Schools of Oriental Research. American Schools of Oriental Research, New Haven.
Lichtenberger, A., Raja, R., 2017. Mosaicists at work: the organisation of Mosaic production in early Islamic Jerash. Antiquity 91, 998–1010.
Lichtenberger, A., Raja, R., 2018a. The Archaeology and History of Jerash: 110 Years of Excavations. Jerash Papers 1. Turnout, Brepols.
Lichtenberger, A., Raja, R., 2018b. Middle Islamic Jerash (9th – 15th Century). Archaeology and History of an Ayyubid-Mamluk Settlement. Jerash Papers 3. Brepols, Turnout.
Lichtenberger, A., Raja, R., 2018c. From synagogue to church. The appropriation of the synagogue of Gerasa/Jerash under Justinian. Jahrb. für Antike Christ. 61, 85–100.
Lichtenberger, A., Raja, R., 2019a. Defining Borders: the Umayyad-abbasid transition and the earthquake of AD 749 in Jerash. In: Lichtenberger, A., Raja, R. (Eds.), Byzantine and Umayyad Jerash Reconsidered. Transitions, Transformations, Continuities. Jerash Papers 4. Brepols, Turnout, pp. 265–286.
Lichtenberger, A., Raja, R., 2019b. Byzantine and Umayyad Jerash Reconsidered. Transitions, Transformations, Continuities. Jerash Papers 4. Brepols, Turnout.
Lichtenberger, A., Raja, R., 2019c. The Danish-German Jerash Northwest Quarter project: results from the 2014-2015 seasons. Stud. Hist. Archaeol. Jordan 12, 51–71.
Lichtenberger, A., Raja, R., 2020. Hellenistic and Roman Gerasa. The Archaeology and History of a Decapolis City. Jerash Papers 5. Brepols. Turnout.
Lichtenberger, A., Raja, R., Eger, C., Kalaitzoglou, G., Højen Sørensen, A., 2016. A newly excavated private house in Jerash. Reconsidering aspects of continuity and change in material culture from Late Antiquity to the early Islamic period. Antiq. Tardive 24, 317–359.
Lichtenberger, A., Raja, R., Seland, E., Kinnaird, T., Simpson, I., 2019. Urban-riverine hinterland synergies in semi-arid environments: millennial-scale change, adaptations and environmental responses at Gerasa/Jerash. J. Field Archaeol. 44, 333–351.
Lichtenberger, A., Raja, R., Seland, E., Simpson, I., 2021. Scaling up and zooming in: global history and high-definition archaeology perspectives on the longue durée of urban-environmental relations in Geresa (Jerash, Jordan). J. Global Hist. 1–20.
Lilyquist, C., Brill, R.H., Brill, R.H., Wypyski, M.T., 1993. Studies in Early Egyptian Glass. Metropolitan Museum of Art.
Maltoni, S., Silvestri, A., Marcante, A., Molin, G., 2016. The transition from roman to late antique glass: new insights from the Domus of Tito macro in Aquileia (Italy). J. Arch. Sci. 73, 1–16.
Marii, F., Rehren, T., 2009. Archaeological coloured glass cakes and tesserae from the Petra Church. AnnAIHV 17, 295–300.
Marii, F., Rehren, T., 2012. Levantine glass of Petra characteristics. AnnAIHV 18, 277–283.
Mirti, P., Davit, P., Gulmini, M., Saguì, L., 2001. Glass fragments from the Crypta Balbi in Rome: the composition of eighth-century fragments. Archaeometry 43, 491–502.
Mirti, P., Pace, M., Negro Ponzi, M.M., Aceto, M., 2008. ICP–MS analysis of glass fragments of parthian and sasanian Epoch from seleucia and Veh Ardašīr (Central Iraq). Archaeometry 50, 429–450.
Mirti, P., Pace, M., Malandrino, M., Negro Ponzi, M.M., 2009. Sasanian glass from Veh Ardasir: new evidences by ICP-MS analysis. J. Arch. Sci. 36, 1061e1069.
Natan, E., Gorin-Rosen, Y., Benzonelli, A., Cvikel, D., 2021. Maritime trade in early Islamic-period glass: new evidence from the Ma'agan Mikhael B shipwreck. J. Arch. Sci. Rep. 37, 102903.
Nielsen, C.H., Sigurdsson, H., 1981. Quantitative methods for electron micro-probe analysis of sodium in natural and synthetic glasses. Am. Mineral. 66, 547–552.
Orfanou, V., Birch, T., Lichtenberger, A., Raja, R., Barfod, G.H., Lesher, C.E., Eger, C., 2020. Copper-based metalwork in Roman to early Islamic Jerash (Jordan): insights into production and recycling through alloy compositions and lead isotopes. J. Arch. Sci. Rep. 33, 102519.
Paynter, S., 2006. Analyses of colourless roman glass from Binchester, county Durham. J. Arch. Sci. 33, 1037–1057.
Paynter, S., 2008. Experiments in the reconstruction of Roman wood-fired glassworking furnaces: waste products and their formation processes. J. Glass Stud. 50, 271–290.
Paynter, S., Kearns, T., Cool, H., Chenery, S., 2015. Roman coloured glass in the Western provinces: the glass cakes and tesserae from West Clacton in England. J. Arch. Sci. 62, 66–81.
Paynter, S., Jackson, C.M., 2016. Re-used roman rubbish: a thousand years of recycling glass. Post-Classical Archaeol. 6, 31–52.
Phelps, M., Freestone, I.C., Gorin-Rosen, Y., Gratuze, B., 2016. Natron glass production and supply in the late antique and early medieval Near East: the effect of the Byzantine-Islamic transition. J. Arch. Sci. 75, 57–71.
Phelps, M., 2018. Glass supply and trade in early Islamic Ramla: an investigation of the plant ash glass. In: Things that Travelled: Mediterranean Glass in the First Millennium CE. UCL Press, London, pp. 236–282.
Raja, R., 2012. Urban Development and Regional Identity in the Eastern Roman Provinces, 50 BC – AD 250: Aphrodisias, Ephesos. Museum Tusculanum Press, Athens, Gerasa.
Rehren, T., Freestone, I.C., 2015. Ancient glass: from kaleidoscope to crystal ball. J. Arch. Sci. 56, 233–241.
Rehren, T., Marii, F., Schibille, N., Stanford, L., Swan, C., 2010. Glass supply and circulation in early Byzantine southern Jordan. In: Drauschke, J., Keller, D. (Eds.), Glas in Byzanz: Produktion, Verwendung, Analysen, Mainz, RGAM Tagungen Band 8, 65–81. Mainz: Verlag des Romisch-Germanischen Zentralmuseums.
Romanowska, I., Brughmans, T., Bes, P., Carrignon, S., Egelund, L., Lichtenberger, A., Raja, R., 2021a. A study of the centuries-long reliance on local ceramics in Jerash through full quantification and simulation. J. Arch. Method. Theor. https://doi.org/10.1007/s10816-021-09510-0.
Romanowska, I., Lichtenberger, A., Raja, R., 2021b. Trends in ceramic assemblages from The northwest Quarter of Gerasa/Jerash, Jordan. J. Arch. Sci. Rep. https://doi.org/10.1016/j.jasrep.2020.102778.
Sainsbury, V., 2018. When things stopped travelling: recycling and the glass industry in Britain from the first to fifth century CE. In: Rosenow, D., Phelps, M., Meek, A., Freestone, I.C. (Eds.), Things that Travelled: Glass in the First Millennium CE. UCL Press, London, pp. 324–345.
Schibille, N., Freestone, I.C., 2013. Composition, production and procurement of glass at san Vincenzo al Volturno: an early medieval monastic complex in southern Italy. PLoS One 8, e76479.
Schibille, N., Gratuze, B., Ollivier, E., Blondeau, E., 2019. Chronology of early Islamic glass compositions from Egypt. J. Archaeol. Sci. 104, 10–18.
Schibille, N., Meek, A., Tobias, B., Entwistle, C., Avisseau-Broustet, M., Da Mota, H., Gratuze, B., 2016. Comprehensive chemical characterisation of Byzantine glass weights. PLoS One 11, e0168289.
Schibille, N., Sterrett-Krause, A., Freestone, I.C., 2017. Glass groups, glass supply and recycling in late Roman Carthage. Archaeol. Anthrop. Sci. 9, 1223–1241.
Silvestri, A., Molin, G., Salviulo, G., 2008. The colourless glass of Iulia Felix. J. Arch. Sci. 35, 331–341.
Silvestri, A., 2008. The coloured glass of Iulia Felix. J. Arch. Sci. 35, 1489–1501.
Stott, D., Kristiansen, S.M., Lichtenberger, A., Raja, R., 2018. Mapping an ancient city with a century of remotely sensed data. P. Natl. Acad. Sci. 115, E5450–E5458.
Tal, O., Jackson-Tal, R.E., Freestone, I.C., 2004. New evidence of the production of raw glass at late Byzantine Apollonia-Arsuf. Israel. J. Glass. Stud. 51–66.
Tal, O., Jackson-Tal, R.E., Freestone, I.C., 2008. Glass from a late Byzantine secondary workshop at Ramla (south), Israel. J. Glass Stud. 81–95.
Walmsley, A.G., 2012. Regional exchange and the role of the shop in Byzantine and early Islamic Syria-Palestine: an archaeological view. In: Trade and Markets in Byzantium. Dumbarton Oaks Research Library and Collection, pp. 311–330.
Weinberg, G.D., 1988. Excavations at Jalame: Site of a Glass Factory in Late Roman Palestine. University of Missouri Press.
Welles, C.B., 1938. The inscriptions. In: Kraeling, C.H. (Ed.), Gerasa, City of the Decapolis: an Account Embodying the Record of a Joint Excavation Conducted by Yale University and the British School of Archaeology in Jerusalem (1928–1930), and Yale University and the American Schools of Oriental Research. American Schools of Oriental Research, New Haven, pp. 353–494.
Whitehouse, D., 2004. Glass in the price edict of Diocletian. J. Glass Stud. 46, 189–191.
Wilson, A., Bowman, A.K., 2018. Trade, Commerce, and the State in the Roman World. Oxford University Press.
Zayadine, F., 1986. Jerash Archaeological Project, I: 1981–1983. Department of Antiquities of Jordan, Amman.

Reference list – Supplementary Tables

Adlington, L.W., 2017. The Corning Archaeological Reference Glasses: New Values for" Old" Compositions, vol. 27. Papers from the Institute of Archaeology.
Brill, R.H., 1999. Chemical Analyses of Early Glasses. Corning. Corning Museum of Glass, NY.
Vicenzi, E.P., Eggins, S., Logan, A., Wysoczanski, R., 2002. Archeological reference glasses: new additions to the smithsonian. J. Res. Natl. Inst. Stan. 107, 719–727.
Wagner, B., Nowak, A., Bulska, E., Hametner, K., Günther, D., 2012. Critical assessment of the elemental composition of Corning archeological reference glasses by LA-ICP-MS. Anal. Bioanal. Chem. 402, 1667–1677.